



Discovery, optimization, and target identification of novel coumarin derivatives as HIV-1 reverse transcriptase-associated ribonuclease H inhibitors



Dongwei Kang^{a,*}, Çağıl Urhan^b, Fenju Wei^a, Estrella Frutos-Beltrán^b, Lin Sun^a, Mar Álvarez^b, Da Feng^a, Yucen Tao^a, Christophe Pannecouque^c, Erik De Clercq^c, Luis Menéndez-Arias^{b,**}, Xinyong Liu^{a,***}, Peng Zhan^{a,****}

^a Department of Medicinal Chemistry, Key Laboratory of Chemical Biology, Ministry of Education, School of Pharmaceutical Sciences, Cheeloo College of Medicine, Shandong University, Ji'nan, 250012, China

^b Centro de Biología Molecular "Severo Ochoa" (Consejo Superior de Investigaciones Científicas & Universidad Autónoma de Madrid), Madrid, Spain

^c Rega Institute for Medical Research, K. U. Leuven, Minderbroedersstraat 10, B-3000, Leuven, Belgium

ARTICLE INFO

Article history:

Received 3 May 2021

Received in revised form

29 July 2021

Accepted 31 July 2021

Available online 11 August 2021

Keywords:

HIV-1

RNase H inhibitor

Coumarin

Phenotypic screen

Drug design

ABSTRACT

Despite significant advances in antiretroviral therapy, acquired immunodeficiency syndrome remains as one of the leading causes of death worldwide. New antiretroviral drugs combined with updated treatment strategies are needed to improve convenience, tolerability, safety, and antiviral efficacy of available therapies. In this work, a focused library of coumarin derivatives was exploited by cell phenotypic screening to discover novel inhibitors of HIV-1 replication. Five compounds (**DW-3**, **DW-4**, **DW-11**, **DW-25** and **DW-31**) showed moderate activity against wild-type and drug-resistant strains of HIV-1 (IIIB and RES056). Four of those molecules were identified as inhibitors of the viral RT-associated RNase H. Structural modification of the most potent **DW-3** and **DW-4** led to the discovery of compound **8a**. This molecule showed increased potency against wild-type HIV-1 strain ($EC_{50} = 3.94 \pm 0.22 \mu\text{M}$) and retained activity against a panel of mutant strains, showing EC_{50} values ranging from 5.62 μM to 202 μM . In enzymatic assays, **8a** was found to inhibit the viral RNase H with an IC_{50} of 12.3 μM . Molecular docking studies revealed that **8a** could adopt a binding mode similar to that previously reported for other active site HIV-1 RNase H inhibitors.

© 2021 Elsevier Masson SAS. All rights reserved.

1. Introduction

Acquired immunodeficiency syndrome (AIDS) is caused by human immunodeficiency virus type 1 (HIV-1), and remains as a major threat to human health worldwide. Currently, the number of people infected with HIV-1 in the world is estimated at 38 million, causing 690,000 deaths due to AIDS in 2019 [1]. Although treatment with potent combination antiretroviral therapies has resulted in major improvements in overall survival, immune function and

the incidence of opportunistic infections, their success is still hampered by their adverse side effects and the emergence of drug resistance [2–4]. Therefore, the development of potent, affordable and highly effective antiretroviral drugs blocking the replication of drug-resistant HIV strains is an important research priority.

Drug discovery through cell-based phenotypic screening has a long track record of delivering innovative drugs and has received renewed attention [5,6]. However, phenotypic screening has also disadvantages, since it is time-consuming, labor intensive and often shows a low success rate. On the other hand, drug repositioning strategies have become increasingly popular, and increasing numbers of approved drugs are being re-evaluated, especially for the development of antiviral drugs [7,8]. Nevertheless, most of the discoveries of new therapeutic uses of existing drugs are based on clinical observations or serendipitous findings.

* Corresponding authors.

** Corresponding author.

*** Corresponding authors.

**** Corresponding author.

E-mail addresses: kangdongwei@sdu.edu.cn (D. Kang), lmendez@cbm.csic.es (L. Menéndez-Arias), xinyongl@sdu.edu.cn (X. Liu), zhanpeng1982@sdu.edu.cn (P. Zhan).

Our labs have been interested in the development of novel inhibitors blocking HIV-1 replication, active against drug-resistant variants, and most notably those emerging during treatment with HIV-1 reverse transcriptase (RT) inhibitors [9–14]. Most of this work was done through rational drug design. Now, we report on the discovery of novel coumarin derivatives with anti-HIV activity through a drug-repositioning strategy.

Coumarin is one of the most common structures found in bioactive molecules. Its derivatives have attracted a lot of attention due to their pharmacological properties as antibacterial [15], antiviral [16] and antitumoral drugs [17,18], as well as their effects promoting lymph circulation and preventing renal failure [19]. Among them, warfarin has been used for over 60 years as anticoagulant and is considered as an essential medicine by the World Health Organization [20]. A more complex coumarin-based natural product known as (+)-calanolide A has been identified as an HIV-1 nonnucleoside RT inhibitor (NNRTI), and developed as antiretroviral agent while completing phase 1 clinical trials [21]. However, its development was extremely slow and eventually halted. In our study, we have identified novel coumarin derivatives targeting the HIV-1 RT-associated RNase H. Optimization *via* structure-based drug design of a series of hit compounds identified through a repositioning strategy led to the identification of a coumarin derivative (compound **8a**) that showed antiviral efficacy against the wild-type HIV-1 strain, as well as a panel of HIV-1 strains bearing mutations associated with resistance to NNRTIs.

2. Results and discussion

2.1. Discovery of coumarin derivatives as novel HIV-1 inhibitors via a phenotypic screen

In a previous project involving the development of anti-renal failure inhibitors, we constructed a mini focused library consisting of ~100 coumarin derivatives [22]. These compounds (structurally related to urolithin A, daphnetin, esculetin or wedelolactone, among others) were expected to act as inhibitors of caspase-dependent apoptosis by regulating the balance between Bcl-2 and Bax expression [17,23,24]. However, as described above, coumarin is a privileged scaffold that targets many biological activities, including antiviral effects against HIV-1, due to the inhibition of various steps of the viral replication cycle (e.g. reverse transcription, integration and maturation) [25–29]. Among them, natural products such as prenylated coumarins of *Antocarpus heterophyllus* or *Clausena lenis* showed EC₅₀ values in the range of 7.4–9.1 μM, although their molecular target was not identified in those studies [30,31]. Esposito et al. [25] obtained a series of substituted coumarin compounds with RNase H inhibitory activity in enzymatic assays. Although most of those compounds showed weak activity, the most potent derivative (i.e., 3-acetyl-4-hydroxy-9-methyl-2*H*,5*H*-pyrano[3,2-*c*]chromene-2,5-dione) showed an

IC₅₀ of 6.75 μM in RNase H inhibition assays. Unfortunately, none of those compounds was active in cell-based assays.

Therefore, following a drug repositioning strategy, the library compounds were screened for their antiviral activity *in vitro* against the wild-type (WT) HIV-1 strain IIB, a double-mutant HIV-1 strain RES056 (K103 N/Y181C) and HIV-2 (ROD strain), and their cellular cytotoxicity was determined using the MTT method [32]. Their antiviral effect in cell culture (EC₅₀; 50% effective concentration) and cytotoxicity (CC₅₀; 50% cytotoxic concentration) were obtained for the synthesized compounds, using the approved NNRTI drug nevirapine (NVP) as reference. Results revealed that five compounds (**DW-3**, **DW-4**, **DW-11**, **DW-25** and **DW-31**) were active against HIV-1 IIB and the NVP-resistant strain RES056, with EC₅₀ values ranging from 19.6 μM to 213 μM (Table 1). All five compounds were particularly effective against both HIV-1 strains, although **DW-3**, **DW-4**, and **DW-25** were also active against the wild-type HIV-2 ROD strain, with EC₅₀ values of 116–144 μM.

Analysis of the structures of **DW-3**, **DW-4**, **DW-11**, **DW-25** and **DW-31** revealed that these molecules contain three main components: a coumarin scaffold (red), an aromatic (dominant) hydrophobic substituent (cyan) and a linker (yellow) (Fig. 1). Based on the current knowledge of the interactions at the catalytic site of RNases H and their inhibitors [33,34], we hypothesized that the coumarin scaffold could be a relevant pharmacophore to inhibit HIV-1 RNase H activity. Therefore, we determined the inhibitory activity of the selected **DW** compounds in enzymatic assays, using as substrate a template-primer containing a 31-nucleotide RNA labeled at its 5' end with ³²P, annealed to a 21-nucleotide DNA [35]. RNA cleavage (in the presence or absence of the candidate inhibitors) was followed by separation of the labeled RNA products by electrophoresis in denaturing polyacrylamide gels and phosphorimaging analysis. The results are shown in Table 1. While **DW-11** (IC₅₀ > 250 μM) failed to inhibit the HIV-1 RNase H activity, related compounds **DW-3**, **DW-4**, **DW-25** and **DW-31** were effective inhibitors. **DW-3** was identified as the most potent, showing an IC₅₀ of 9.9 μM.

The stronger RNase H inhibitory activity of **DW-3** and **DW-4** in comparison with **DW-25** and **DW-31** was not reflected in the EC₅₀ values obtained in cell-based assays. This phenomenon has been previously observed with other antiretroviral drug candidates [10,14,36] and could be attributed to a decreased cell permeability of **DW-3** and **DW-4**. In addition, these compounds contain multiple hydrogen bond donor and acceptor atoms that could favor the formation of cocrystals and salts, thereby reducing their bioavailability.

Guided by the pharmacophore model of HIV-1 RNase H inhibitors, three novel series of coumarinamide derivatives were designed and synthesized with **DW-3**, **DW-4**, **DW-11**, **DW-25** and **DW-31** as leads, with the aim to discover more potent HIV-1 RNase H inhibitors. As shown in Fig. 1, the newly designed derivatives retained the privileged divalent metal ion chelating group and linker, while exploring elaborated structural modifications of the

Table 1
Antiviral activity and cytotoxicity in MT-4 cells, and RNase H inhibitory activity of representative compounds of the DW series.

Compounds	EC ₅₀ (μM) ^a			CC ₅₀ (μM) ^b	HIV-1 RNase HIC ₅₀ (μM) ^c
	IIB	ROD	RES056		
DW-3	121 ± 10.5	121 ± 22.4	113 ± 3.65	>312	9.90 ± 1.50
DW-4	101 ± 9.12	116 ± 9.37	107 ± 3.58	>310	20.8 ± 5.7
DW-11	208 ± 56.1	>280	213 ± 55.1	>280	>250
DW-25	28.5 ± 7.10	144 ± 37.3	19.6 ± 0.52	>271	45.1 ± 15.0
DW-31	82.7 ± 9.44	>231	123 ± 15.4	>231	68.5 ± 33.3
NVP	0.28 ± 0.04	ND ^d	>15.02	>15.02	ND ^d

^a EC₅₀: concentration of the compound required to achieve 50% protection of MT-4 cell cultures against HIV-1-induced cytopathicity, as determined using the MTT method.

^b CC₅₀: concentration required to reduce the viability of mock-infected cell cultures by 50%, as determined using the MTT method.

^c IC₅₀: Concentration required to inhibit by 50% the *in vitro* RNase H activity.

^d ND, not determined.

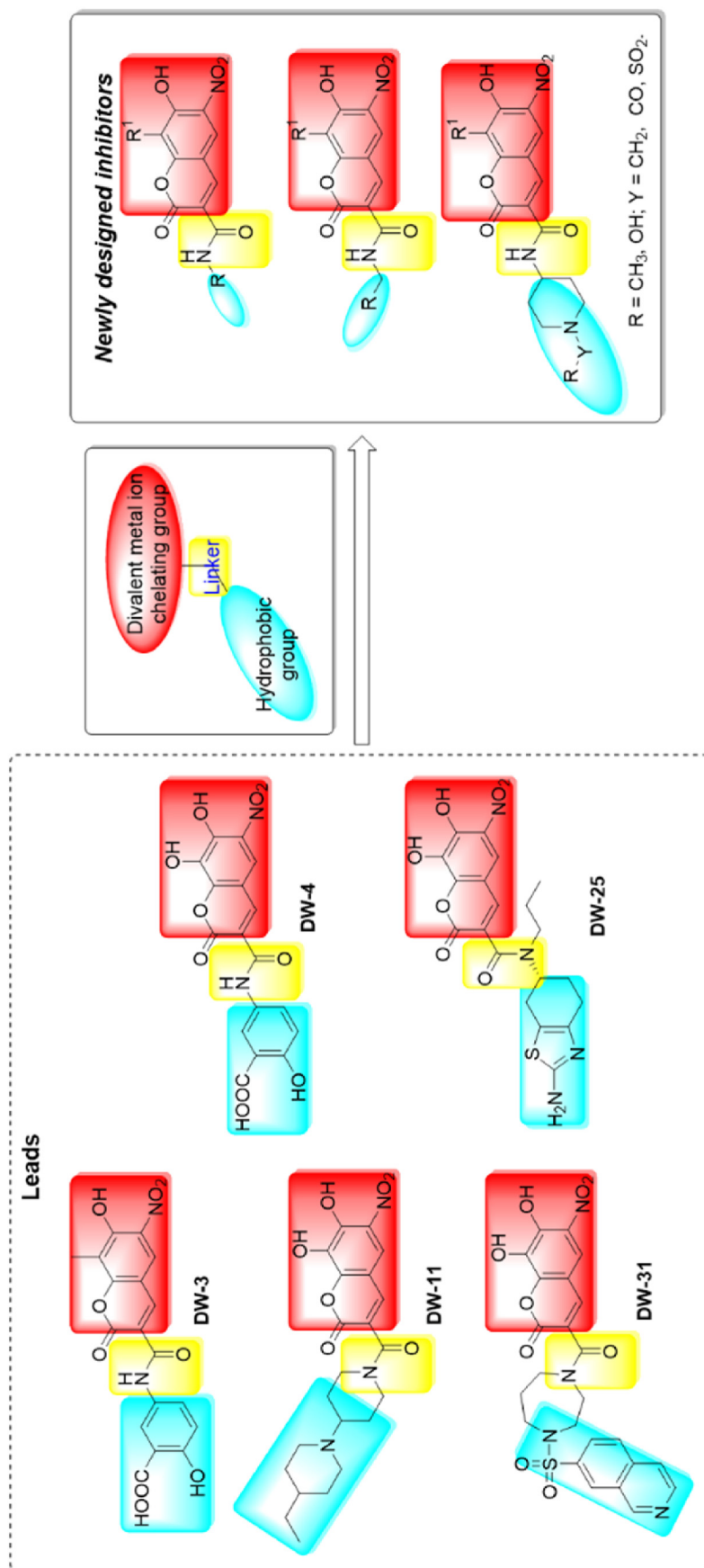
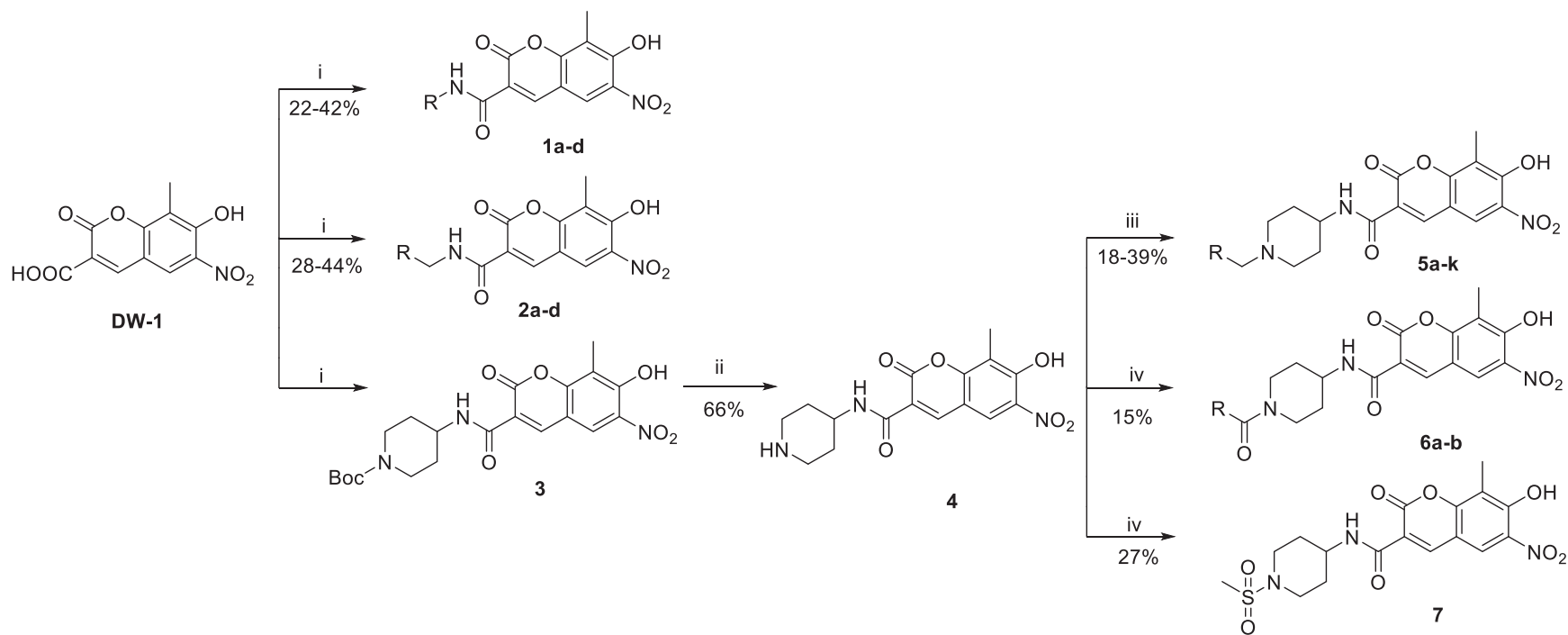
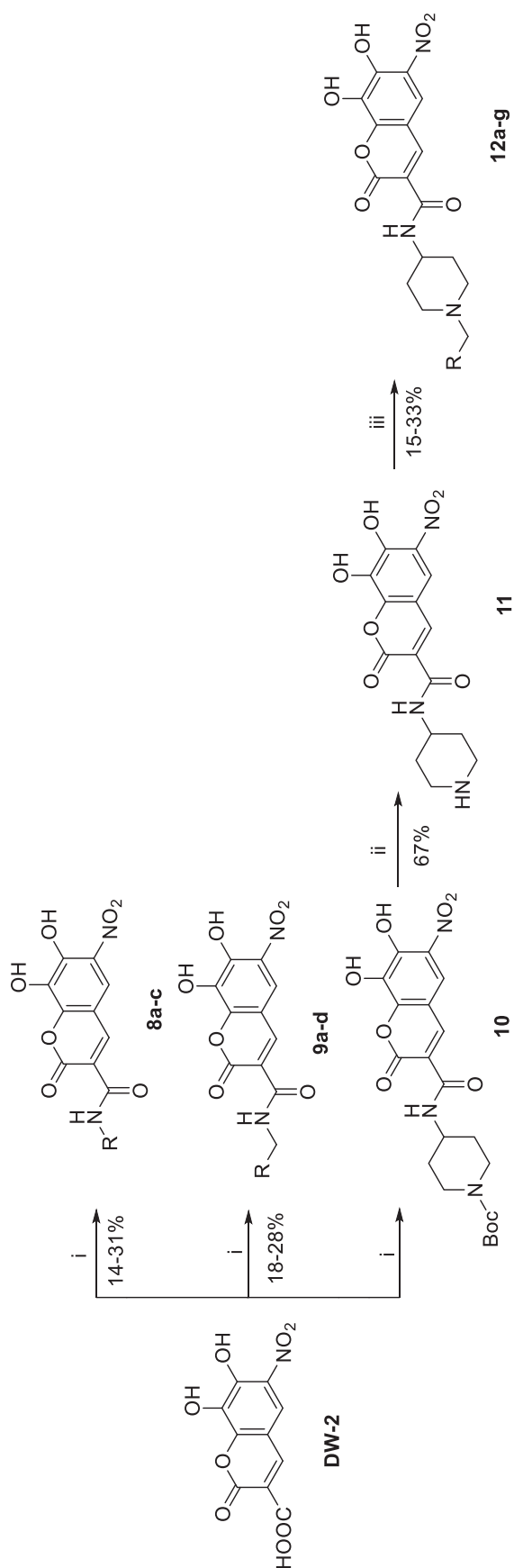


Fig. 1. Structure of the leads (DW series) and newly designed inhibitors.





Scheme 2. Reagents and conditions: (i) HATU, K_2CO_3 , DMF, r.t.; (ii) TFA, DCM, r.t.; (iii) K_2CO_3 , DMF, r.t.

hydrophobic pocket by introducing structural diversity groups, such as substituted anilines, substituted benzylamines and substituted piperylhydrazines.

2.2. Optimization of compound **8a** as a novel HIV-1 RNase H inhibitor

The target compounds were prepared via a concise synthetic route as outlined in Schemes 1 and 2. The starting material **DW-1** was reacted with different anilines, benzylamines and *tert*-butyl 4-aminopiperidine-1-carboxylate to form target compounds **1a-d**, **2a-d**, and intermediate **3**, respectively. Then, **3** was treated with trifluoroacetic acid to give the key intermediate **4**. Subsequent treatment of **4** with substituted benzyl bromide, substituted acyl chloride and dimethylsulfamoyl chloride rendered target compounds **5a-k**, **6a-b** and **7**, respectively (Scheme 1). In an analogous way, target compounds **8a-c**, **9a-d**, and **12a-g** were prepared, only with the difference that the starting material was **DW-2** (Scheme 2).

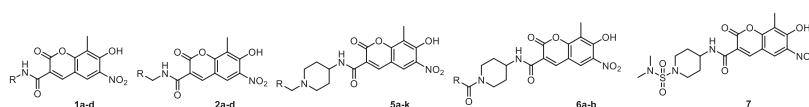
As shown in Table 2, when R is a CH_3 group, all compounds of the **1**, **2** and **6** subseries showed no antiviral activity against HIV-1 IIIB in cell culture at their highest tested concentrations. Three compounds of the **5** subseries (**5c**, **5e** and **5f**) exhibited moderate potency against HIV-1 IIIB (EC_{50} = 167 μ M, 234 μ M, and 138 μ M, respectively), with similar efficacy in comparison with the lead compound **DW-3**. In addition, **5c** was also effective against HIV-2 ROD, showing an EC_{50} value of 148 μ M. However, their antiviral activity was much lower than that of the approved drug NVP (EC_{50} = 0.09 μ M).

Newly designed compounds containing an OH group at position 8 of the chromenone ring (i.e. compounds **8a**, **8c**, **9d**, **12c** and **12e**) showed moderate inhibitory activity of the replication of HIV-1 IIIB, with EC_{50} values within 3.94 and 237 μ M (Table 3). Among them, compound **8a** turned out to be the most potent inhibitor, exhibiting an EC_{50} value of 3.94 μ M, about 25 times more potent than the lead **DW-4** (EC_{50} = 101.15 μ M). For HIV-2 ROD, compound **8a** (EC_{50} = 169 μ M) exhibited comparable activity with that of **DW-4** (EC_{50} = 116 μ M). In addition, **8a** exhibited no cytotoxicity at the highest tested concentrations (CC_{50} > 300 μ M). Besides, the activity of compound **9d** (EC_{50} = 46.1 μ M) was also superior to that of **DW-4**. Although it was difficult to establish a clear structure-activity relationship for these novel compounds, it is clear that an OH group at position 8 of the chromenone ring would be more beneficial to improve the antiviral activity.

Compounds **DW-4** and **8a** differ at the substituent group on the benzene ring which is $COOH$ in **DW-4** and CO_2CH_3 in **8a**. Differences in antiviral activity between both inhibitors could be attributed to their cellular permeability. Although both compounds showed relatively low permeability in Caco-2 cells, obtained values were higher for compound **8a** (P_{app} = 9.06×10^{-6} cm/s) than for **DW-4** (P_{app} = 5.71×10^{-6} cm/s), thereby suggesting that this property is an important contributor to the stronger antiviral effect of **8a** in cell culture.


Compound **8a** was further tested against a panel of mutant HIV-1 strains, including NNRTI-resistant variants containing amino acid substitutions in the viral RT, such as L100I, K103 N, Y181C, Y188L, E138K, V106A/F227L, and RES056. As shown in Table 4, the compound exhibited some activity against all mutant strains, with EC_{50} values ranging from 5.62 μ M to 202 μ M. Interestingly, compound **8a** was found to be a weak but effective inhibitor of NVP-resistant variants such as Y188L and V106A/F227L, as well as the RES056 strain. These results demonstrated that **8a** could be regarded as a promising lead compound for further structural modification to discover novel potent inhibitors with improved drug resistance profiles.

Table 2
Structure, antiviral activity against HIV-1 IIIB and HIV-2 ROD, and cytotoxicity of target compounds **1a-d**, **2a-d**, **5a-k**, **6a-b** and **7**.



Compounds	Structure	EC ₅₀ (μM) ^a		CC ₅₀ (μM) ^b
		III _B	ROD	
1a		>182	>182	182 ± 90.3
1b		>6.50	>6.50	6.50 ± 2.84
1c		>12.5	>12.5	12.5 ± 2.82
1d		>10.7	>10.7	10.7 ± 3.05
2a		>44.0	>44.0	44.0 ± 8.31
2b		>47.5	>47.5	47.5 ± 16.4
2c		>45.0	>45.0	45.0 ± 11.6
2d		>32.5	>32.5	32.5 ± 17.0
5a		>7.80	>7.80	7.80 ± 7.19
5b		>42.6	>42.6	42.6 ± 4.72
5c		167 ± 82.5	148 ± 15.0	>264
5d		>72.3	>72.3	72.3 ± 52.9
5e		234 ± 18.1	>259	>259
5f		138 ± 25.9	>260	>260
5g		>276	>276	>276
5h		>3.88	>3.88	3.88 ± 0.69
5i		>50.5	>50.5	50.5 ± 41.2
5j		>9.38	>9.38	9.37 ± 1.26
5k		>14.7	>14.7	14.7 ± 3.22
6a		>251	>251	>251

Table 2 (continued)

Compounds	Structure	EC ₅₀ (μM) ^a		CC ₅₀ (μM) ^b
		III _B	ROD	
6b		>19.9	>19.9	19.9 ± 6.60
7	—	>50.8	>50.8	50.8 ± 9.87
NVP	—	1.9 ± 0.01	ND ^c	>15.0
DW3	—	121 ± 10.5	121 ± 22.4	>312

^a EC₅₀: concentration of the compound required to achieve 50% protection of MT-4 cell cultures against HIV-1-induced cytopathicity, as determined using the MTT method.

^b CC₅₀: concentration required to reduce the viability of mock-infected cell cultures by 50%, as determined using the MTT method.

^c ND, not determined.

2.3. HIV-1 RNase H inhibition and mechanism of action of compound 8a

Representative compounds of the newly synthesized compounds were tested *in vitro* for their inhibitory activity against the RNase H of HIV-1 RT (Table 5). The initial screening at 100 μM showed that compounds **1c**, **2c**, **5c**, **9a** and **12b** had less than 50% inhibitory activity at that concentration. Most of the other compounds were classified as weak inhibitors, with IC₅₀s above 50 μM. Among them, **5f**, **12g**, **12a** and **8c** were the most potent and showed 37.1, 32.4, 31.8 and 12.0% inhibition at such a concentration. In contrast, the inhibitory effect of compounds **5h**, **5k**, **8b**, **9d** and **12f** was almost negligible at 50 μM concentration (<10% inhibition).

Interestingly, the inhibitory activity of compounds **8a** and **12a** was similar to that of the lead compound **DW-3**, with IC₅₀ values around 10 μM. As discussed above, compound **8a** was the most potent antiviral molecule in antiviral assays, while **12a** showed important cellular toxicity and was not effective in cell culture.

Further insight into the mechanism of action of compound **8a** was obtained from molecular docking studies of this molecule in the HIV-1 RNase H catalytic site, using the Schrödinger software and the crystal structure of HIV-1 RT bound to 5-hydroxy-4-oxo-1-[(4'-sulfamoyl[1,1'-biphenyl]-4-yl)methyl]-1,4-dihydropyridine-3-carboxylic acid, an RNase H inhibitor with sub-micromolar efficacy in enzymatic assays [37].

As depicted in Fig. 2, the predicted binding mode of **8a** was similar to that previously reported for other HIV-1 RNase H inhibitors. According to the obtained models, the two phenolic hydroxyl groups and the nitril moiety of compound **8a** could chelate the two Mg²⁺ ions, which are coordinated to the conserved active site acidic residues Asp443, Glu478, Asp498 and Asp549, and required for RNase H activity. In addition, the hydroxyl group located in the hydrophobic phenyl ring and in a distal location relative to the active site of the RNase H could establish hydrogen bond interactions with the side-chain of Lys540. Docking accuracy was rather good, since a root mean square deviation (RMSD) value of 1.08 Å was obtained between the docked conformation of the inhibitor and the active ligand conformation found in the crystal structure (PDB file 5J1E).

Docking results were also consistent with the experimental observations showing that **8a** is a potent HIV-1 RNase H inhibitor, validating the advantages of ambident scaffolds in metal ion chelating and providing a basis for further rational drug optimization.

3. Conclusion

To discover new potent HIV-1 inhibitors with novel mechanisms of action and scaffolds, a mini focused library of coumarin derivatives was screened for anti-HIV-1 activity through a drug repositioning strategy. Preliminary phenotypic screening results at

the cellular level demonstrated that five compounds (**DW-3**, **DW-4**, **DW-11**, **DW-25** and **DW-31**) exhibited moderate potency (EC₅₀ values within 19.6 and 213 μM) against HIV-1 III_B and the NNRTI-resistant strain RES056. These compounds were then identified as HIV-1 RNase H inhibitors after being tested in enzymatic assays using RNA-DNA template-primers as substrates. Further optimization of **DW-3** and **DW-4** led to the discovery of compound **8a** which showed similar inhibitory potency than **DW-3** in *in vitro* RNase H activity assays, but an increased antiviral effect against HIV-1 III_B and a panel of mutant strains bearing amino acid substitutions associated with resistance to NNRTIs. Molecular docking studies of **8a** bound to HIV-1 RT revealed that the compound could adopt a binding mode similar to that previously reported for other active site HIV-1 RNase H inhibitors.

4. Experimental section

4.1. Chemistry

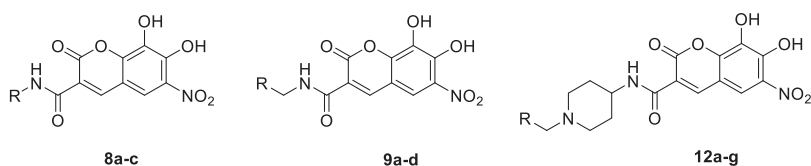
All melting points were determined on a micro melting point apparatus and are uncorrected. ¹H NMR spectra were recorded in DMSO-*d*₆ on a Bruker AV-400 spectrometer with tetramethylsilane (TMS) as the internal standard. A G1313A Standard LC Autosampler (Agilent) was used to collect samples for measurement of mass spectra. All reactions were monitored by thin layer chromatography (TLC), and spots were visualized with iodine vapor or by irradiation with UV light. Flash column chromatography was performed on columns packed with Silica Gel (200–300 mesh). Solvents were of reagent grade and were purified by standard methods when necessary.

4.1.1. General procedure for the preparation of target compounds 1a-d and 2a-d

A solution of starting material **DW-1** (0.10 g, 0.377 mmol) and 2-(7-azabenzotriazol-1-yl)-*N,N,N',N'*-tetramethyluronium hexafluorophosphate (HATU) (0.21 g, 0.566 mmol) in DMF (4 mL) was stirred at room temperature for 10 min; then K₂CO₃ (0.052 g, 0.377 mmol) and different anilines or benzylamines (0.377 mmol) were added, and the mixture was stirred for another 5–10 h (monitored by thin layer chromatography). The solvent was removed under reduced pressure and 30 mL water was added to the residue. Then the mixture solution was extracted with ethyl acetate and washed with saturated sodium chloride, purified by flash column chromatography and recrystallized from ethyl acetate (EA)/petroleum ether (PE) to afford the target compounds **1a-d** and **2a-d**.

4.1.1.1. Methyl 2-hydroxy-5-(7-hydroxy-8-methyl-6-nitro-2-oxo-2H-chromene-3-carboxamido)benzoate (**1a**). **1a** was synthesized from **DW-1** (0.1 g, 0.377 mmol), K₂CO₃ (52 mg, 0.377 mmol), HATU (215 mg, 0.566 mmol), and methyl 5-amino-2-hydroxybenzoate

Table 3
Structure, antiviral activity against HIV-1 IIIB and HIV-2 ROD, and cytotoxicity of target compounds **8a-c**, **9a-d**, and **12a-g**.



Compounds	Structure	EC ₅₀ (μM) ^a		CC ₅₀ (μM) ^b
		III _B	ROD	
8a		3.94 ± 0.22	169 ± 17.4	>300
8b		>200	>200	200 ± 39.0
8c		237 ± 17.2	>330	>330
9a		>272	>272	272 ± 10.0
9b		>228	>228	228 ± 33.2
9c		>259	>259	259 ± 39.7
9d		46.1 ± 14.0	>266	266 ± 17.5
12a		>21.7	>21.7	21.7 ± 4.60
12b		>112	>112	112 ± 58.2
12c		160 ± 77.3	>269	>269
12d		≥101	>217	≥217
12e		210 ± 47.5	>220	≥220
12f		>143	>143	143 ± 45.7
12g		>153	>153	153 ± 50.6
NVP	—	0.09 ± 0.01	ND ^c	>15.0
DW-4	—	101 ± 9.12	116 ± 9.37	>310

^a EC₅₀: concentration of the compound required to achieve 50% protection of MT-4 cell cultures against HIV-1-induced cytopathicity, as determined using the MTT method.

^b CC₅₀: concentration required to reduce the viability of mock-infected cell cultures by 50%, as determined using the MTT method.

^c ND, not determined.

Table 4
Activity against mutant HIV-1 strains of compound **8a** and NVP.

Cpds	EC ₅₀ (μM) ^a						
	L100I	K103 N	Y181C	Y188L	E138K	V106A/F227	RES056
8a	16.5 ± 0.79	5.62 ± 1.99	22.4 ± 4.40	44.3 ± 8.96	22.5 ± 4.40	101 ± 48.7	202 ± 61.2
NVP	0.70 ± 0.29	2.85 ± 0.37	4.09 ± 0.65	≥2.97	0.12 ± 0.04	≥5.78	>9.51

^a EC₅₀: concentration of the compound required to achieve 50% protection of MT-4 cell cultures against HIV-1-induced cytopathicity, as determined using the MTT method.

Table 5
HIV-1 RNase H inhibitory activity of selected compounds.

Compounds	IC ₅₀ (µM) ^a	Compounds	IC ₅₀ (µM) ^a
1c	>100 (28.6)	9a	>100 (48.0)
2c	>100 (38.7)	9d	>50 (68.6)
5c	>100 (23.8)	12a	8.4 ± 2.7
5f	>50 (87.2)	12b	>100 (47.4)
5h	>50 (72.1)	12e	>50 (57.7)
5i	45.2 ± 8.8	12f	>50 (72.5)
5k	>50 (62.9)	12g	>50 (57.4)
8a	12.3 ± 2.8	DW-3	9.9 ± 1.5
8b	>50 (72.5)	DW-4	20.8 ± 5.7
8c	>50 (78.0)		

^a Concentration required to inhibit by 50% the *in vitro* RNase H activity. Numbers between parentheses indicate the maximum percent inhibition observed with the corresponding coumarinamide derivative at 100 µM concentration (reported values are averages of two independent determinations).

(63 mg, 0.377 mmol). Yellow solid, 22% yield, carbonize at 320 °C. ¹H NMR (400 MHz, DMSO-*d*₆) δ 10.45 (s, 1H, NH), 8.89 (s, 1H, CH), 8.68 (s, 1H, Ph-H), 8.26 (d, *J* = 2.6 Hz, 1H, Ph-H), 7.76 (dd, *J* = 8.9, 2.7 Hz, 1H, Ph-H), 7.02 (d, *J* = 8.9 Hz, 1H, Ph-H), 3.93 (s, 3H, CH₃), 2.30 (s, 3H, CH₃). HRMS *m/z* C₁₉H₁₄N₂O₉: calcd 414.0699, found 413.1054 [M – H][–].

4.1.1.2. N-(4-fluorophenyl)-7-hydroxy-8-methyl-6-nitro-2-oxo-2H-chromene-3-carboxamide(1b). **1b** was synthesized from **DW-1** (0.1 g, 0.377 mmol), K₂CO₃ (52 mg, 0.377 mmol), HATU (215 mg, 0.566 mmol), and 4-fluoroaniline (36 µL, 0.377 mmol). Brick red solid, 40% yield, carbonize at 280 °C. ¹H NMR (400 MHz, DMSO-*d*₆) δ 10.54 (s, 1H, NH), 8.84 (s, 1H, CH), 8.56 (s, 1H, Ph-H), 7.72 (s, 2H, Ph-H), 7.20 (s, 2H, Ph-H), 2.23 (s, 3H, CH₃). ¹³C NMR (100 MHz, DMSO-*d*₆) δ 160.9, 160.5, 160.1, 158.8, 157.7, 155.8, 148.1, 135.7, 134.9, 126.2, 122.2 (*J*_{CF} = 8.0 Hz), 116.1 (*J*_{CF} = 22.0 Hz), 115.4, 113.8, 109.5, 9.0. HRMS *m/z* C₁₇H₁₁FN₂O₆: calcd 358.0601, found 357.0842 [M – H][–].

4.1.1.3. N-(3-fluorophenyl)-7-hydroxy-8-methyl-6-nitro-2-oxo-2H-chromene-3-carboxamide(1c). **1c** was synthesized from **DW-1** (0.1 g, 0.377 mmol), K₂CO₃ (52 mg, 0.377 mmol), HATU (215 mg, 0.566 mmol), and 3-fluoroaniline (36 µL, 0.377 mmol). Yellow solid, 37% yield, carbonize at 300 °C. ¹H NMR (400 MHz, DMSO-*d*₆) δ 10.71 (s, 1H, NH), 8.86 (s, 1H, CH), 8.61 (s, 1H, Ph-H), 7.74 (d, *J* = 11.2 Hz, 1H, Ph-H), 7.51–7.34 (m, 2H, Ph-H), 7.04–6.87 (m, 1H, Ph-H), 2.28 (s, 3H, CH₃). ¹³C NMR (100 MHz, DMSO-*d*₆) δ 163.8 (*J*_{CF} = 241 Hz),

160.8, 160.1, 156.0, 147.8, 140.1, 135.1, 131.1 (*J*_{CF} = 9.0 Hz), 125.8, 117.5, 116.2 (*J*_{CF} = 3.0 Hz), 115.5, 111.2, 110.8, 107.3, 9.1. HRMS *m/z* C₁₇H₁₁FN₂O₆: calcd 358.0601, found 357.1124 [M – H][–].

4.1.1.4. N-(2-fluorophenyl)-7-hydroxy-8-methyl-6-nitro-2-oxo-2H-chromene-3-carboxamide(1d). **1d** was synthesized from **DW-1** (0.1 g, 0.377 mmol), K₂CO₃ (52 mg, 0.377 mmol), HATU (215 mg, 0.566 mmol), and 2-fluoroaniline (36 µL, 0.377 mmol). Yellow solid, 42% yield, carbonize at 280 °C. ¹H NMR (400 MHz, DMSO-*d*₆) δ 10.84 (s, 1H, NH), 9.01 (s, 1H, CH), 8.66 (s, 1H, Ph-H), 8.36 (t, *J* = 7.7 Hz, 1H, Ph-H), 7.40–7.28 (m, 1H, Ph-H), 7.28–7.12 (m, 2H, Ph-H), 2.27 (s, 3H, CH₃). ¹³C NMR (100 MHz, DMSO-*d*₆) δ 161.5, 160.1, 156.0 (*J*_{CF} = 194 Hz), 149.0, 135.6, 126.6 (*J*_{CF} = 10 Hz), 126.2, 125.4, 125.4, 125.3, 122.1, 115.8 (*J*_{CF} = 19 Hz), 110.6, 9.1. HRMS *m/z* C₁₇H₁₁FN₂O₆: calcd 358.0601, found 357.1584 [M – H][–].

4.1.1.5. N-(4-fluorobenzyl)-7-hydroxy-8-methyl-6-nitro-2-oxo-2H-chromene-3-carboxamide(2a). **2a** was synthesized from **DW-1** (0.1 g, 0.377 mmol), K₂CO₃ (52 mg, 0.377 mmol), HATU (215 mg, 0.566 mmol), and (4-fluorophenyl)methanamine (43 µL, 0.377 mmol). Yellow solid, 43% yield, mp: 234–236 °C. ¹H NMR (400 MHz, DMSO-*d*₆) δ 9.00 (t, *J* = 5.9 Hz, 1H, NH), 8.87 (s, 1H, CH), 8.64 (s, 1H, Ph-H), 7.39 (dd, *J* = 8.1, 5.8 Hz, 2H, Ph-H), 7.15 (t, *J* = 8.8 Hz, 2H, Ph-H), 4.51 (d, *J* = 6.0 Hz, 2H, CH₂), 2.26 (s, 3H, CH₃). HRMS *m/z* C₁₈H₁₃FN₂O₆: calcd 372.0758, found 371.0028 [M – H][–].

4.1.1.6. N-(3-fluorobenzyl)-7-hydroxy-8-methyl-6-nitro-2-oxo-2H-chromene-3-carboxamide(2b). **2b** was synthesized from **DW-1** (0.1 g, 0.377 mmol), K₂CO₃ (52 mg, 0.377 mmol), HATU (215 mg, 0.566 mmol), and (3-fluorophenyl)methanamine (43 µL, 0.377 mmol). Yellow solid, 32% yield, mp: 235–236 °C. ¹H NMR (400 MHz, DMSO-*d*₆) δ 9.05 (t, *J* = 5.9 Hz, 1H, NH), 8.87 (s, 1H, CH), 8.65 (s, 1H, Ph-H), 7.37 (q, *J* = 7.7 Hz, 1H, Ph-H), 7.17 (t, *J* = 9.4 Hz, 2H, Ph-H), 7.07 (t, *J* = 8.6 Hz, 1H, Ph-H), 4.55 (d, *J* = 6.0 Hz, 2H, CH₂), 2.27 (s, 3H, CH₃). HRMS *m/z* C₁₈H₁₃FN₂O₆: calcd 372.0758, found 371.1425 [M – H][–].

4.1.1.7. N-(2-fluorobenzyl)-7-hydroxy-8-methyl-6-nitro-2-oxo-2H-chromene-3-carboxamide(2c). **2c** was synthesized from **DW-1** (0.1 g, 0.377 mmol), K₂CO₃ (52 mg, 0.377 mmol), HATU (215 mg, 0.566 mmol), and (2-fluorophenyl)methanamine (43 µL, 0.377 mmol). Yellow solid, 28% yield, carbonize at 220 °C. ¹H NMR (400 MHz, DMSO-*d*₆) δ 9.00 (t, *J* = 5.9 Hz, 1H, NH), 8.88 (s, 1H, CH), 8.66 (s, 1H, Ph-H), 7.39 (t, *J* = 7.6 Hz, 1H, Ph-H), 7.33 (q, *J* = 5.9 Hz,

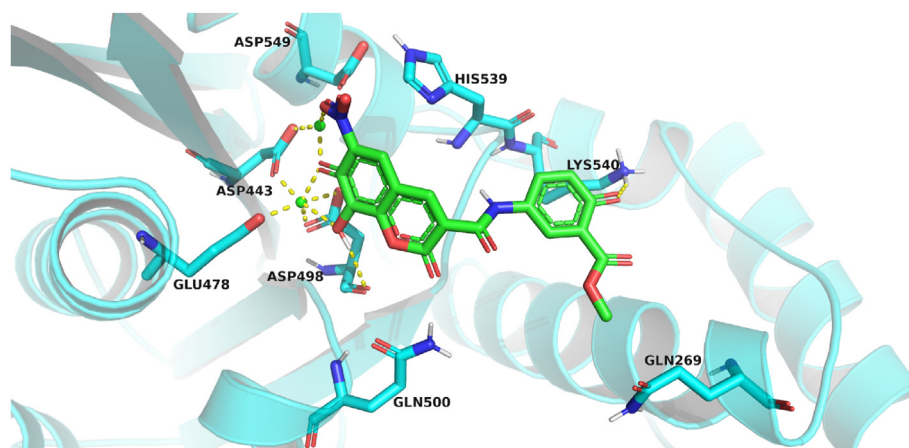


Fig. 2. Predicted binding modes of **8a** (green) in the HIV-1 RNase H active site (PDB code: 5J1E [37]). Protein carbon atoms are shown in cyan, hydrogen bonds between **8a** and amino acid residues are indicated with dashed lines (yellow). Figures were prepared with the PyMOL visualization program (<http://www.pymol.org>).

1H, Ph-H), 7.19 (q, $J = 9.4, 7.6$ Hz, 2H, Ph-H), 4.59 (d, $J = 5.9$ Hz, 2H, CH₂), 2.27 (s, 3H, CH₃). ¹³C NMR (100 MHz, DMSO-*d*₆) δ 161.7, 160.2, 159.3, 156.2, 154.9, 147.9, 134.3, 129.9, 129.5 ($J_{CF} = 8.0$ Hz), 126.1, 125.9 ($J_{CF} = 3.0$ Hz), 124.8, 117.6, 115.7 ($J_{CF} = 21$ Hz), 115.3, 111.6, 37.3, 8.9. HRMS m/z C₁₈H₁₃FN₂O₆: calcd 372.0758, found 371.1125 [M – H][–].

4.1.1.8. *N*-(2-chloro-4-fluorobenzyl)-7-hydroxy-8-methyl-6-nitro-2-oxo-2H-chromene-3-carboxamide(2d). **2d** was synthesized from **DW-1** (0.1 g, 0.377 mmol), K₂CO₃ (52 mg, 0.377 mmol), HATU (215 mg, 0.566 mmol), and (2-chloro-4-fluorophenyl)methanamine (36 μ L, 0.377 mmol). Yellow solid, 44% yield, carbonize at 260 °C. ¹H NMR (400 MHz, DMSO-*d*₆) δ 9.06 (s, 1H, NH), 8.87 (s, 1H, CH), 8.64 (s, 1H, Ph-H), 7.64–7.31 (m, 2H, Ph-H), 7.29–7.07 (m, 1H, Ph-H), 4.86–4.35 (m, 2H, CH₂), 2.26 (s, 3H, CH₃). ¹³C NMR (100 MHz, DMSO-*d*₆) δ 162.7, 161.7 ($J_{CF} = 185$ Hz), 160.2, 156.2, 155.6, 148.0, 134.5, 133.2, 132.8, 130.9 ($J_{CF} = 9.0$ Hz), 125.8, 117.0 ($J_{CF} = 4.0$ Hz), 116.8, 115.4, 114.8 ($J_{CF} = 21$ Hz), 111.3, 40.7, 9.1. HRMS m/z C₁₈H₁₂ClFN₂O₆: calcd 406.0368, found 405.1320 [M – H][–].

4.1.1.9. *tert*-butyl 4-(7-hydroxy-8-methyl-6-nitro-2-oxo-2H-chromene-3-carboxamido)piperidine-1-carboxylate(3). A solution of **DW-1** (0.10 g, 0.377 mmol) and HATU (0.21 g, 0.566 mmol) in DMF (4 mL) was stirred at room temperature for 10 min; then K₂CO₃ (0.052 g, 0.377 mmol) and *tert*-butyl 4-aminopiperidine-1-carboxylate (76 mg, 0.377 mmol) were added, and the mixture was stirred for another 4 h. The solvent was removed under reduced pressure and 30 mL water was added. Then the solution was extracted with ethyl acetate and washed with saturated sodium chloride, purified by flash column chromatography and recrystallized from EA/PE to afford the target compound **3** as a yellow solid in 43% yield. ESI-MS: 446.32 [M – H][–]. C₂₁H₂₅N₃O₈ [447.16].

4.1.1.10. 7-hydroxy-8-methyl-6-nitro-2-oxo-*N*-(piperidin-4-yl)-2H-chromene-3-carboxamide(4). To a solution of **3** (0.45 g, 1.0 mmol) in dichloromethane (DCM) (4 mL) was added trifluoroacetic acid (TFA) (0.74 mL, 10 mmol) at room temperature, and the mixture was stirred for 5 h (monitored by TLC). Then, the reaction solution was alkalinized to pH 9 with saturated sodium bicarbonate solution and extracted with DCM. The organic layer was washed with brine, dried over anhydrous Na₂SO₄, filtered and concentrated under reduced pressure to give **4** as a yellow solid in 66% yield. ESI-MS: 346.41 [M – H][–]. C₁₆H₁₇N₃O₆ [347.11].

4.1.2. General procedure for the preparation of target compounds 5a-k

To a solution of **4** (0.35 g, 1.0 mmol) in anhydrous DMF (10 mL) was added K₂CO₃ (0.28 g, 2.0 mmol) and substituted benzyl bromine (1.2 mmol), and the solution was stirred for 4–7 h (monitored by TLC) at room temperature. The solvent was removed under reduced pressure and 30 mL water was added to the residue. Then the mixture solution was extracted with ethyl acetate and washed with saturated sodium chloride, purified by flash column chromatography and recrystallized from EA/PE to afford the target compounds **5a-k**.

4.1.2.1. *N*-(1-benzylpiperidin-4-yl)-7-hydroxy-8-methyl-6-nitro-2-oxo-2H-chromene-3-carboxamide(5a). **5a** was synthesized from **4** (0.1 g, 0.288 mmol), K₂CO₃ (80 mg, 0.576 mmol), and (bromomethyl)benzene (41 μ L, 0.346 mmol). Brick red solid, 20% yield, carbonize at 240 °C. ¹H NMR (400 MHz, DMSO-*d*₆) δ 8.59 (d, $J = 7.2$ Hz, 1H, NH), 8.53 (s, 1H, CH), 8.14 (s, 1H, Ph-H), 7.55–7.40 (m, 5H, Ph-H), 4.23 (s, 2H, CH₂), 4.07–3.92 (m, 1H, CH), 3.24–3.16 (m, 2H, CH₂), 3.11–3.00 (m, 2H, CH₂), 2.06 (d, $J = 13.4$ Hz, 2H, CH₂), 1.98

(s, 3H, CH₃), 1.88–1.65 (m, 2H, CH₂). HRMS m/z C₂₃H₂₃N₃O₆: calcd 437.1587, found 436.0745 [M – H][–].

4.1.2.2. *N*-(1-(4-fluorobenzyl)piperidin-4-yl)-7-hydroxy-8-methyl-6-nitro-2-oxo-2H-chromene-3-carboxamide(5b). **5b** was synthesized from **4** (0.1 g, 0.288 mmol), K₂CO₃ (80 mg, 0.576 mmol), and 1-(bromomethyl)-4-fluorobenzene (43 μ L, 0.346 mmol). Orange solid, 24% yield, carbonize at 245 °C. ¹H NMR (400 MHz, DMSO-*d*₆) δ 8.58 (d, $J = 7.1$ Hz, 1H, NH), 8.54 (s, 1H, CH), 8.16 (s, 1H, Ph-H), 7.53 (dd, $J = 8.2, 5.7$ Hz, 2H, Ph-H), 7.30 (t, $J = 8.7$ Hz, 2H, Ph-H), 4.22 (s, 2H, CH₂), 4.06–3.92 (m, 1H, CH), 3.24 (d, $J = 11.2$ Hz, 2H, CH₂), 3.07–2.95 (m, 2H, CH₂), 2.05 (d, $J = 12.3$ Hz, 2H, CH₂), 1.99 (s, 3H, CH₃), 1.84–1.63 (m, 2H, CH₂). ¹³C NMR (100 MHz, DMSO-*d*₆) δ 167.4, 164.2, 162.6 ($J_{CF} = 16$ Hz), 161.8, 155.1, 148.9, 138.5, 133.7, 133.6, 127.2, 116.2 ($J_{CF} = 21$ Hz), 115.3, 107.1, 104.3, 50.6, 44.3, 9.0. HRMS m/z C₂₃H₂₂FN₃O₆: calcd 455.1493, found 454.1029 [M – H][–].

4.1.2.3. *N*-(1-(4-chlorobenzyl)piperidin-4-yl)-7-hydroxy-8-methyl-6-nitro-2-oxo-2H-chromene-3-carboxamide(5c). **5c** was synthesized from **4** (0.1 g, 0.288 mmol), K₂CO₃ (80 mg, 0.576 mmol), and 1-(bromomethyl)-4-chlorobenzene (45 μ L, 0.346 mmol). Orange solid, 25% yield, carbonize at 260 °C. ¹H NMR (400 MHz, DMSO-*d*₆) δ 8.57 (d, $J = 7.3$ Hz, 1H, NH), 8.55 (s, 1H, CH), 8.18 (s, 1H, Ph-H), 7.59–7.43 (m, 4H, Ph-H), 4.19 (s, 2H, CH₂), 4.04–3.92 (m, 1H, CH), 3.22 (d, $J = 11.7$ Hz, 2H, CH₂), 2.99 (t, $J = 11.0$ Hz, 2H, CH₂), 2.10–2.02 (m, 2H, CH₂), 1.99 (s, 3H, CH₃), 1.84–1.65 (m, 2H, CH₂). ¹³C NMR (100 MHz, DMSO-*d*₆) δ 167.0, 162.5, 162.3, 155.2, 148.8, 138.3, 134.4, 133.1, 130.8, 129.2, 127.1, 115.3, 107.6, 104.6, 58.6, 50.7, 44.4, 29.1, 9.07. HRMS m/z C₂₃H₂₂ClN₃O₆: calcd 471.1197, found 470.1523 [M – H][–].

4.1.2.4. *N*-(1-(4-bromobenzyl)piperidin-4-yl)-7-hydroxy-8-methyl-6-nitro-2-oxo-2H-chromene-3-carboxamide(5d). **5d** was synthesized from **4** (0.1 g, 0.288 mmol), K₂CO₃ (80 mg, 0.576 mmol), and 1-bromo-4-(bromomethyl)benzene (48 μ L, 0.346 mmol). Orange solid, 39% yield, carbonize at 245 °C. ¹H NMR (400 MHz, DMSO-*d*₆) δ 8.57 (d, $J = 7.4$ Hz, 1H, NH), 8.55 (s, 1H, CH), 8.18 (s, 1H, Ph-H), 7.66 (d, $J = 8.3$ Hz, 2H, Ph-H), 7.43 (d, $J = 8.3$ Hz, 2H, Ph-H), 4.17 (s, 2H, CH₂), 4.04–3.92 (m, 1H, CH), 3.21 (d, $J = 11.3$ Hz, 2H, CH₂), 2.97 (t, $J = 10.8$ Hz, 2H, CH₂), 2.10–2.01 (m, 2H, CH₂), 1.99 (s, 3H, CH₃), 1.83–1.66 (m, 2H, CH₂). HRMS m/z C₂₃H₂₂BrN₃O₆: calcd 515.0692, found 514.1020 [M – H][–].

4.1.2.5. 7-hydroxy-8-methyl-6-nitro-*N*-(1-(4-nitrobenzyl)piperidin-4-yl)-2-oxo-2H-chromene-3-carboxamide(5e). **5e** was synthesized from **4** (0.1 g, 0.288 mmol), K₂CO₃ (80 mg, 0.576 mmol), and 1-(bromomethyl)-4-nitrobenzene (45 μ L, 0.346 mmol). Orange solid, 19% yield, carbonize at 250 °C. ¹H NMR (400 MHz, DMSO-*d*₆) δ 8.54 (s, 1H, CH), 8.51 (d, $J = 7.2$ Hz, 1H, NH), 8.23 (d, $J = 8.5$ Hz, 2H, Ph-H), 8.20 (s, 1H, Ph-H), 7.67 (d, $J = 8.5$ Hz, 2H, Ph-H), 4.13 (s, 2H, CH₂), 3.93–3.82 (m, 1H, CH), 3.06 (d, $J = 12.6$ Hz, 2H, CH₂), 2.81 (d, $J = 12.4$ Hz, 2H, CH₂), 1.98 (s, 3H, CH₃), 1.96–1.87 (m, 2H, CH₂), 1.73–1.58 (m, 2H, CH₂). HRMS m/z C₂₃H₂₂N₄O₈: calcd 482.1438, found 481.1007 [M – H][–].

4.1.2.6. *N*-(1-(4-carbamoylbenzyl)piperidin-4-yl)-7-hydroxy-8-methyl-6-nitro-2-oxo-2H-chromene-3-carboxamide(5f). **5f** was synthesized from **4** (0.1 g, 0.288 mmol), K₂CO₃ (80 mg, 0.576 mmol), and 4-(bromomethyl)benzamide (47 μ L, 0.346 mmol). Orange solid, 22% yield, carbonize at 205 °C. ¹H NMR (400 MHz, DMSO-*d*₆) δ 8.58 (d, $J = 7.2$ Hz, 1H, NH), 8.54 (s, 1H, CH), 8.17 (s, 1H, Ph-H), 8.02 (s, 1H, NH), 7.93 (d, $J = 8.1$ Hz, 2H, Ph-H), 7.56 (d, $J = 8.1$ Hz, 2H, Ph-H), 7.43 (s, 1H, NH), 4.21 (s, 2H, CH₂), 4.02–3.93 (m, 1H, CH), 3.21 (d, $J = 11.1$ Hz, 2H, CH₂), 2.97 (t, $J = 10.8$ Hz, 2H, CH₂), 2.11–2.00 (m, 2H, CH₂), 1.99 (s, 3H, CH₃), 1.83–1.68 (m, 2H,

CH₂). ¹³C NMR (100 MHz, DMSO-*d*₆) δ 167.8, 162.5, 162.4, 157.2, 155.1, 148.9, 138.5, 135.2, 130.9, 128.2, 127.2, 115.3, 107.1, 104.2, 102.9, 98.6, 75.6, 29.2, 9.0. HRMS *m/z* C₂₄H₂₄N₄O₇: calcd 480.1645, found 479.1126 [M – H][–].

4.1.2.7. 7-hydroxy-8-methyl-N-(1-(4-methylbenzyl)piperidin-4-yl)-6-nitro-2-oxo-2H-chromene-3-carboxamide(5g). **5g** was synthesized from **4** (0.1 g, 0.288 mmol), K₂CO₃ (80 mg, 0.576 mmol), and 1-(bromomethyl)-4-methylbenzene (47 μL, 0.346 mmol). Orange solid, 29% yield, carbonize at 220 °C. ¹H NMR (400 MHz, DMSO-*d*₆) δ 8.58 (d, *J* = 7.7 Hz, 1H, NH), 8.52 (s, 1H), 8.13 (s, 1H, CH), 7.37 (d, *J* = 7.9 Hz, 2H, Ph-H), 7.28 (d, *J* = 7.9 Hz, 2H, Ph-H), 4.21 (s, 2H, CH₂), 4.06–3.91 (m, 1H, CH), 3.29–3.20 (m, 2H, CH₂), 3.13–2.99 (m, 2H, CH₂), 2.33 (s, 3H, CH₃), 2.13–2.01 (m, 2H, CH₂), 1.97 (s, 3H, CH₃), 1.86–1.65 (m, 2H, CH₂). HRMS *m/z* C₂₄H₂₅N₃O₆: calcd 451.1743, found 450.1338 [M – H][–].

4.1.2.8. 7-hydroxy-8-methyl-N-(1-(3-methylbenzyl)piperidin-4-yl)-6-nitro-2-oxo-2H-chromene-3-carboxamide(5h). **5h** was synthesized from **4** (0.1 g, 0.288 mmol), K₂CO₃ (80 mg, 0.576 mmol), and 1-(bromomethyl)-3-methylbenzene (47 μL, 0.346 mmol). Orange solid, 18% yield, mp: 170–172 °C. ¹H NMR (400 MHz, DMSO-*d*₆) δ 8.58 (d, *J* = 6.3 Hz, 1H, NH), 8.53 (s, 1H, CH), 8.14 (s, 1H, Ph-H), 7.35 (t, *J* = 7.4 Hz, 1H, Ph-H), 7.28 (dd, *J* = 11.7, 6.2 Hz, 3H, Ph-H), 4.19 (s, 2H, CH₂), 4.04–3.91 (m, 1H, CH), 3.29–3.23 (m, 2H, CH₂), 3.10–3.00 (m, 2H, CH₂), 2.34 (s, 3H, CH₃), 2.10–2.02 (m, 2H, CH₂), 1.97 (s, 3H, CH₃), 1.82–1.68 (m, 2H, CH₂). HRMS *m/z* C₂₄H₂₅N₃O₆: calcd 451.1743, found 450.1097 [M – H][–].

4.1.2.9. N-(1-(3-fluorobenzyl)piperidin-4-yl)-7-hydroxy-8-methyl-6-nitro-2-oxo-2H-chromene-3-carboxamide(5i). **5i** was synthesized from **4** (0.1 g, 0.288 mmol), K₂CO₃ (80 mg, 0.576 mmol), and 1-(bromomethyl)-3-fluorobenzene (43 μL, 0.346 mmol). Orange solid, 22% yield, carbonize at 210 °C. ¹H NMR (400 MHz, DMSO-*d*₆) δ 8.58 (d, *J* = 7.5 Hz, 1H, NH), 8.51 (s, 1H, CH), 8.11 (s, 1H, Ph-H), 7.56–7.51 (m, 1H, Ph-H), 7.46 (d, *J* = 7.8 Hz, 1H, Ph-H), 7.37–7.27 (m, 2H, Ph-H), 3.87–3.73 (m, 1H, CH), 3.53 (s, 2H, CH₂), 2.78–2.64 (m, 2H, CH₂), 2.22 (t, *J* = 9.6 Hz, 2H, CH₂), 1.96 (s, 3H, CH₃), 1.91–1.81 (m, 2H, CH₂), 1.59–1.44 (m, 2H, CH₂). ¹³C NMR (100 MHz, DMSO-*d*₆) δ 169.5, 162.8, 162.4, 155.0, 149.1, 138.8, 136.1, 133.6, 131.8, 131.4, 130.3, 128.3, 127.5, 122.0, 115.3, 106.0, 103.2, 61.4, 51.7, 45.9, 31.8, 9.1. HRMS *m/z* C₂₃H₂₂FN₃O₆: calcd 455.1493, found 454.1023 [M – H][–].

4.1.2.10. N-(1-(3-chlorobenzyl)piperidin-4-yl)-7-hydroxy-8-methyl-6-nitro-2-oxo-2H-chromene-3-carboxamide(5j). **5j** was synthesized from **4** (0.1 g, 0.288 mmol), K₂CO₃ (80 mg, 0.576 mmol), and 1-(bromomethyl)-3-chlorobenzene (45 μL, 0.346 mmol). Orange solid, 24% yield, carbonize at 240 °C. ¹H NMR (400 MHz, DMSO-*d*₆) δ 8.58 (d, *J* = 7.8 Hz, 1H, NH), 8.57 (s, 1H, CH), 8.20 (s, 1H, Ph-H), 7.58 (s, 1H, Ph-H), 7.49 (d, *J* = 6.8 Hz, 2H, Ph-H), 7.45 (t, *J* = 6.2 Hz, 1H, Ph-H), 4.19 (s, 2H, CH₂), 4.05–3.92 (m, 1H, CH), 3.23 (d, *J* = 11.5 Hz, 2H, CH₂), 2.99 (t, *J* = 10.9 Hz, 2H, CH₂), 2.11–2.03 (m, 2H, CH₂), 2.00 (s, 3H, CH₃), 1.75 (q, *J* = 10.1 Hz, 2H, CH₂). HRMS *m/z* C₂₃H₂₂ClN₃O₆: calcd 471.1197, found 470.0852 [M – H][–].

4.1.2.11. N-(1-(3-bromobenzyl)piperidin-4-yl)-7-hydroxy-8-methyl-6-nitro-2-oxo-2H-chromene-3-carboxamide(5k). **5k** was synthesized from **4** (0.1 g, 0.288 mmol), K₂CO₃ (80 mg, 0.576 mmol), and 1-bromo-3-(bromomethyl)benzene (55 μL, 0.346 mmol). Orange solid, 18% yield, carbonize at 240 °C. ¹H NMR (400 MHz, DMSO-*d*₆) δ 8.59 (d, *J* = 7.0 Hz, 1H, NH), 8.56 (s, 1H, CH), 8.19 (s, 1H, Ph-H), 7.51 (q, *J* = 7.8 Hz, 1H, Ph-H), 7.39–7.24 (m, 3H, Ph-H), 4.19 (s, 2H, CH₂), 4.03–3.92 (m, 1H, CH), 3.21 (d, *J* = 12.3 Hz, 2H, CH₂), 3.03–2.90 (m,

2H, CH₂), 2.09–2.01 (m, 2H, CH₂), 2.00 (s, 3H, CH₃), 1.83–1.67 (m, 2H, CH₂). HRMS *m/z* C₂₃H₂₂BrN₃O₆: calcd 515.0692, found 514.1120 [M – H][–].

4.1.3. General procedure for the preparation of target compounds **6a–b** and **7**

To a solution of **4** (0.35 g, 1.0 mmol) and Et₃N (0.20 g, 2.0 mmol) in anhydrous DMF (10 mL) was added substituted acyl chloride or dimethylsulfamoyl chloride (1.2 mmol), and the solution was stirred for 3–5 h (monitored by TLC) at room temperature. Then 30 mL water was added, and the mixture was extracted with ethyl acetate and washed with saturated sodium chloride. Purified by flash column chromatography and recrystallized from EA/PE to afford the target compounds **6a–b** and **7**.

4.1.3.1. 7-hydroxy-8-methyl-6-nitro-N-(1-(4-nitrobenzoyl)piperidin-4-yl)-2-oxo-2H-chromene-3-carboxamide(6a). **6a** was synthesized from **4** (0.1 g, 0.288 mmol), Et₃N (80 μL, 0.576 mmol), and 4-nitrobenzoyl chloride (42 μL, 0.346 mmol). Yellow solid, 15% yield, carbonize at 270 °C. ¹H NMR (400 MHz, DMSO-*d*₆) δ 8.87 (s, 1H, CH), 8.65 (s, 1H, Ph-H), 8.53 (d, *J* = 7.7 Hz, 1H, NH), 8.30 (d, *J* = 8.7 Hz, 2H, Ph-H), 7.70 (d, *J* = 8.7 Hz, 2H, Ph-H), 4.44–4.33 (m, 1H, CH), 3.30–3.02 (m, 4H, CH₂ × 2), 2.27 (s, 3H, CH₃), 2.01–1.79 (m, 2H, CH₂), 1.67–1.52 (m, 2H, CH₂). HRMS *m/z* C₂₃H₂₀N₄O₉: calcd 496.1230, found 495.1007 [M – H][–].

4.1.3.2. 4-(7-hydroxy-8-methyl-6-nitro-2-oxo-2H-chromene-3-carboxamido)-N,N-dimethylpiperidine-1-carboxamide(6b). **6b** was synthesized from **4** (0.1 g, 0.288 mmol), Et₃N (80 μL, 0.576 mmol), and methyl dimethylcarbamoyl chloride (32 μL, 0.346 mmol). Brown solid, 15% yield, mp: 246–248 °C. ¹H NMR (400 MHz, DMSO-*d*₆) δ 8.86 (s, 1H, CH), 8.65 (s, 1H, Ph-H), 8.49 (d, *J* = 7.7 Hz, 1H, NH), 4.06–3.91 (m, 1H, CH), 3.48 (d, *J* = 13.3 Hz, 2H, CH₂), 2.91–2.82 (m, 2H, CH₂), 2.74 (s, 6H, CH₃ × 2), 2.26 (s, 3H, CH₃), 1.93–1.78 (m, 2H, CH₂), 1.57–1.39 (m, 2H, CH₂). HRMS *m/z* C₁₉H₂₂N₄O₇: calcd 418.1488, found 417.1224 [M – H][–].

4.1.3.3. N-(1-(N,N-dimethylsulfamoyl)piperidin-4-yl)-7-hydroxy-8-methyl-6-nitro-2-oxo-2H-chromene-3-carboxamide(7). **7** was synthesized from **4** (0.1 g, 0.288 mmol), Et₃N (80 μL, 0.576 mmol), and dimethylsulfamoyl chloride (37 μL, 0.346 mmol). Brown solid, 27% yield, mp: 230–232 °C. ¹H NMR (400 MHz, DMSO-*d*₆) δ 8.85 (d, *J* = 5.6 Hz, 1H, NH), 8.64 (s, 1H, CH), 8.52 (s, 1H, Ph-H), 4.29–4.14 (m, 1H, CH), 3.60–3.40 (m, 4H, CH₂ × 2), 2.76 (s, 6H, CH₃ × 2), 2.26 (s, 3H, CH₃), 2.08–1.82 (m, 2H, CH₂), 1.71–1.48 (m, 2H, CH₂). HRMS *m/z* C₁₈H₂₂N₄O₈: calcd 454.1158, found 453.0885 [M – H][–].

4.1.4. General procedure for the preparation of target compounds **8a–c** and **9a–d**

The synthetic route was similar to that of **1a–d**, only with the difference that the starting material was **DW-2** (0.10 g, 0.377 mmol)

4.1.4.1. Methyl 5-(7,8-dihydroxy-6-nitro-2-oxo-2H-chromene-3-carboxamido)-2-hydroxy benzoate(8a). **8a** was synthesized from **DW-2** (0.1 g, 0.375 mmol), K₂CO₃ (52 mg, 0.375 mmol), HATU (215 mg, 0.563 mmol), and methyl 5-amino-2-hydroxybenzoate (63 mg, 0.375 mmol). Brown solid, 14% yield, carbonize at 250 °C. ¹H NMR (400 MHz, DMSO-*d*₆) δ 10.58 (d, *J* = 15.9 Hz, 1H, NH), 8.91–8.66 (m, 1H, CH), 8.32–8.19 (m, 1H, Ph-H), 8.08–7.96 (m, 1H, Ph-H), 7.83–7.69 (m, 1H, Ph-H), 6.98 (d, *J* = 7.9 Hz, 1H, Ph-H), 3.91 (s, 3H, CH₃). HRMS *m/z* C₁₈H₁₂N₂O₁₀: calcd 416.0492, found 415.0217 [M – H][–].

4.1.4.2. *N*-(4-fluorophenyl)-7,8-dihydroxy-6-nitro-2-oxo-2H-chromene-3-carboxamide(8b). **8b** was synthesized from **DW-2** (0.1 g, 0.375 mmol), K₂CO₃ (52 mg, 0.375 mmol), HATU (215 mg, 0.563 mmol), and 4-fluoroaniline (42 mg, 0.375 mmol). Brown solid, 31% yield, carbonize at 170 °C. ¹H NMR (400 MHz, DMSO-*d*₆) δ 10.47 (s, 1H, NH), 8.81 (s, 1H, CH), 8.42 (s, 1H, Ph-H), 7.76–7.70 (m, 2H, Ph-H), 7.23–7.17 (m, 2H, Ph-H). HRMS *m/z* C₁₆H₉FN₂O₇: calcd 360.0394, found 359.1042 [M – H][–].

4.1.4.3. *N*-(2,4-difluorophenyl)-7,8-dihydroxy-6-nitro-2-oxo-2H-chromene-3-carboxamide(8c). **8c** was synthesized from **DW-2** (0.1 g, 0.375 mmol), K₂CO₃ (52 mg, 0.375 mmol), HATU (215 mg, 0.563 mmol), and 2,4-difluoroaniline (48 mg, 0.375 mmol). Yellow solid, 24% yield, carbonize at 160 °C. ¹H NMR (400 MHz, DMSO-*d*₆) δ 10.72 (s, 1H, NH), 8.87 (s, 1H, CH), 8.45 (s, 1H, Ph-H), 7.51 (dd, *J* = 8.2, 4.2 Hz, 2H, Ph-H), 7.45–7.34 (m, 1H, Ph-H), 7.12 (t, *J* = 8.3 Hz, 1H, Ph-H). HRMS *m/z* C₁₆H₈F₂N₂O₇: calcd 378.0300, found 377.0745 [M – H][–].

4.1.4.4. *N*-(4-fluorobenzyl)-7,8-dihydroxy-6-nitro-2-oxo-2H-chromene-3-carboxamide(9a). **9a** was synthesized from **DW-2** (0.1 g, 0.375 mmol), K₂CO₃ (52 mg, 0.375 mmol), HATU (215 mg, 0.563 mmol), and (4-fluorophenyl)methanamine (43 μL, 0.375 mmol). Yellow solid, 18% yield, carbonize at 180 °C. ¹H NMR (400 MHz, DMSO-*d*₆) δ 8.89 (t, *J* = 6.0 Hz, 1H, NH), 8.73 (s, 1H, CH), 8.37 (s, 1H, Ph-H), 7.37 (dd, *J* = 8.3, 5.8 Hz, 2H, Ph-H), 7.15 (t, *J* = 8.8 Hz, 2H, Ph-H), 4.49 (d, *J* = 6.0 Hz, 2H, CH₂). HRMS *m/z* C₁₇H₁₁FN₂O₇: calcd 374.0550, found 373.0126 [M – H][–].

4.1.4.5. *N*-(3-fluorobenzyl)-7,8-dihydroxy-6-nitro-2-oxo-2H-chromene-3-carboxamide(9b). **9b** was synthesized from **DW-2** (0.1 g, 0.375 mmol), K₂CO₃ (52 mg, 0.375 mmol), HATU (215 mg, 0.563 mmol), and (3-fluorophenyl)methanamine (43 μL, 0.375 mmol). Yellow solid, 19% yield, carbonize at 180 °C. ¹H NMR (400 MHz, DMSO-*d*₆) δ 8.95 (t, *J* = 6.0 Hz, 1H, NH), 8.73 (s, 1H, CH), 8.37 (s, 1H, Ph-H), 7.37 (q, *J* = 7.7 Hz, 1H, Ph-H), 7.15 (t, *J* = 10.3 Hz, 2H, Ph-H), 7.11–7.02 (m, 1H, Ph-H), 4.53 (d, *J* = 6.1 Hz, 2H, CH₂). HRMS *m/z* C₁₇H₁₁FN₂O₇: calcd 374.0500, found 373.2558 [M – H][–].

4.1.4.6. *N*-(2-fluorobenzyl)-7,8-dihydroxy-6-nitro-2-oxo-2H-chromene-3-carboxamide(9c). **9c** was synthesized from **DW-2** (0.1 g, 0.375 mmol), K₂CO₃ (52 mg, 0.375 mmol), HATU (215 mg, 0.563 mmol), and (2-fluorophenyl)methanamine (43 μL, 0.375 mmol). Yellow solid, 21% yield, carbonize at 220 °C. ¹H NMR (400 MHz, DMSO-*d*₆) δ 8.88 (t, *J* = 6.0 Hz, 1H, NH), 8.73 (s, 1H, CH), 8.37 (s, 1H, Ph-H), 7.37 (t, *J* = 7.7 Hz, 1H, Ph-H), 7.34–7.28 (m, 1H, Ph-H), 7.18 (q, *J* = 8.9, 7.3 Hz, 2H, Ph-H), 4.56 (d, *J* = 5.9 Hz, 2H, CH₂). ¹³C NMR (100 MHz, DMSO-*d*₆) δ 162.8 (*J*_{CF} = 155 Hz), 160.9, 159.4, 149.8, 146.8, 138.0, 132.5, 130.0 (*J*_{CF} = 5.0 Hz), 129.5 (*J*_{CF} = 8.0 Hz), 127.1, 126.4 (*J*_{CF} = 15 Hz), 124.8 (*J*_{CF} = 3.0 Hz), 115.7 (*J*_{CF} = 21 Hz), 108.6, 101.9, 37.1, 14.5. HRMS *m/z* C₁₇H₁₁FN₂O₇: calcd 374.0500, found 373.2014 [M – H][–].

4.1.4.7. *N*-(2-chloro-4-fluorobenzyl)-7,8-dihydroxy-6-nitro-2-oxo-2H-chromene-3-carboxamide(9d). **9d** was synthesized from **DW-2** (0.1 g, 0.375 mmol), K₂CO₃ (52 mg, 0.375 mmol), HATU (215 mg, 0.563 mmol), and (2-chloro-4-fluorophenyl)methanamine (47 μL, 0.375 mmol). Orange solid, 28% yield, mp: 180–182 °C. ¹H NMR (400 MHz, DMSO-*d*₆) δ 9.08 (t, *J* = 5.9 Hz, 1H, NH), 8.81 (s, 1H, CH), 8.18 (s, 1H, Ph-H), 7.57–7.50 (m, 1H, Ph-H), 7.46–7.42 (m, 1H, Ph-H), 7.24–7.19 (m, 1H, Ph-H), 4.57 (d, *J* = 6.0 Hz, 2H, CH₂). HRMS *m/z* C₁₆H₈F₂N₂O₇: calcd 408.0161, found 407.3325 [M – H][–].

4.1.4.8. *tert*-butyl(4-(7,8-dihydroxy-6-nitro-2-oxo-2H-chromene-3-carboxamido) piperidine-1-carboxylate(10). The synthetic route

was similar to that of **3**, only with the difference that the starting material was **DW-2** (0.10 g, 0.377 mmol). Yellow solid, 49% yield, carbonize at 270 °C. ¹H NMR (400 MHz, DMSO-*d*₆) δ 8.80 (s, 1H, CH), 8.49 (d, *J* = 7.7 Hz, 1H, NH), 8.19 (s, 1H, Ph-H), 4.06–3.90 (m, 2H, CH₂), 3.90–3.72 (m, 3H, CH₂ + CH), 3.03–2.91 (m, 2H, CH₂), 1.93–1.79 (m, 2H, CH₂), 1.41 (s, 9H, CH₃ × 3). ESI-MS: 448.57 [M – H][–]. C₂₀H₂₃N₃O₉ [449.14].

4.1.4.9. 7,8-Dihydroxy-6-nitro-2-oxo-*N*-(piperidin-4-yl)-2H-chromene-3-carboxamide(11). The synthetic route was similar to that of **4**, only with the difference that the starting material was **10** (0.45 g, 1.0 mmol). Yellow solid, 67% yield, carbonize at 300 °C. ESI-MS: 348.38 [M – H][–]. C₁₅H₁₅N₃O₇ [349.09].

4.1.5. General procedure for the preparation of target compounds 12a-g

The synthetic route was similar to that of **5a-k**, only with the difference that the starting material was **11** (0.35 g, 1.0 mmol).

4.1.5.1. *N*-(1-(4-chlorobenzyl)piperidin-4-yl)-7,8-dihydroxy-6-nitro-2-oxo-2H-chromene-3-carboxamide(12a). **12a** was synthesized from **11** (0.1 g, 0.286 mmol), K₂CO₃ (79 mg, 0.572 mmol), and 1-(bromomethyl)-4-chlorobenzene (45 μL, 0.344 mmol). Brick red solid, 33% yield, carbonize at 180 °C. ¹H NMR (400 MHz, DMSO-*d*₆) δ 8.55 (s, 1H, CH), 8.41 (d, *J* = 7.2 Hz, 1H, NH), 7.94 (s, 1H, Ph-H), 7.50–7.48 (m, 4H, Ph-H), 4.14–4.10 (m, 2H, CH₂), 3.95 (s, 1H, CH), 3.10–3.04 (m, 2H, CH₂), 2.93–2.86 (m, 2H, CH₂), 2.01–1.97 (m, 2H, CH₂), 1.72–1.67 (m, 2H, CH₂). ¹³C NMR (100 MHz, DMSO-*d*₆) δ 162.8, 162.4, 161.9, 149.7, 146.7, 139.8, 136.6, 135.5, 132.8, 130.2, 129.1, 128.8, 127.1, 120.9, 108.6, 104.1, 101.9, 72.0, 50.9, 38.7, 9.1. HRMS *m/z* C₂₂H₂₀ClN₃O₇: calcd 473.0990, found 473.0115 [M – H][–].

4.1.5.2. *N*-(1-(4-bromobenzyl)piperidin-4-yl)-7,8-dihydroxy-6-nitro-2-oxo-2H-chromene-3-carboxamide(12b). **12b** was synthesized from **11** (0.1 g, 0.286 mmol), K₂CO₃ (79 mg, 0.572 mmol), and 1-bromo-4-(bromomethyl)benzene (47 μL, 0.344 mmol). Orange solid, 16% yield, carbonize at 190 °C. ¹H NMR (400 MHz, DMSO-*d*₆) δ 8.70 (s, 1H, CH), 8.40 (d, *J* = 7.5 Hz, 1H, NH), 8.36 (s, 1H, Ph-H), 7.52 (d, *J* = 7.9 Hz, 2H, Ph-H), 7.29 (d, *J* = 7.8 Hz, 2H, Ph-H), 3.86–3.74 (m, 1H, CH), 3.57–3.41 (m, 2H, CH₂), 2.80–2.63 (m, 2H, CH₂), 2.29–2.09 (m, 2H, CH₂), 1.95–1.78 (m, 2H, CH₂), 1.60–1.42 (m, 2H, CH₂). HRMS *m/z* C₂₂H₂₀BrN₃O₇: calcd 517.0485, found 516.0226 [M – H][–].

4.1.5.3. *N*-(1-(4-cyanobenzyl)piperidin-4-yl)-7,8-dihydroxy-6-nitro-2-oxo-2H-chromene-3-carboxamide(12c). **12c** was synthesized from **11** (0.1 g, 0.286 mmol), K₂CO₃ (79 mg, 0.572 mmol), and 4-(bromomethyl)benzotrile (67 mg, 0.344 mmol). Orange solid, 15% yield, carbonize at 220 °C. ¹H NMR (400 MHz, DMSO-*d*₆) δ 8.70 (s, 1H, CH), 8.41 (d, *J* = 7.6 Hz, 1H, NH), 8.36 (s, 1H, Ph-H), 7.81 (d, *J* = 7.8 Hz, 2H, Ph-H), 7.54 (d, *J* = 7.9 Hz, 2H, Ph-H), 3.88–3.78 (m, 1H, CH), 3.72–3.56 (m, 2H, CH₂), 2.83–2.71 (m, 2H, CH₂), 2.37–2.17 (m, 2H, CH₂), 1.91–1.80 (m, 2H, CH₂), 1.58–1.47 (m, 2H, CH₂). HRMS *m/z* C₂₃H₂₀N₄O₇: calcd 464.1332, found 463.1044 [M – H][–].

4.1.5.4. *N*-(1-(4-cyanobenzyl)piperidin-4-yl)-7,8-dihydroxy-6-nitro-2-oxo-2H-chromene-3-carboxamide(12d). **12d** was synthesized from **11** (0.1 g, 0.286 mmol), K₂CO₃ (79 mg, 0.572 mmol), and 1-(bromomethyl)-4-nitrobenzene (74 mg, 0.344 mmol). Brick red solid, 25% yield, carbonize at 160 °C. ¹H NMR (400 MHz, DMSO-*d*₆) δ 8.71 (s, 1H, CH), 8.42 (d, *J* = 7.2 Hz, 1H, NH), 8.37 (s, 1H, Ph-H), 8.26–8.19 (m, 2H, Ph-H), 7.70–7.61 (m, 2H, Ph-H), 3.87 (s, 1H, CH), 3.85–3.74 (m, 2H, CH₂), 2.91–2.79 (m, 2H, CH₂), 2.46–2.33 (m, 2H, CH₂), 1.92 (t, *J* = 12.2 Hz, 2H, CH₂), 1.61 (t, *J* = 17.0 Hz, 2H, CH₃). HRMS *m/z* C₂₂H₂₀N₄O₉: calcd 484.1230, found 483.0021 [M – H][–].

4.1.5.5. *N*-(1-(3-fluorobenzyl)piperidin-4-yl)-7,8-dihydroxy-6-nitro-2-oxo-2H-chromene-3-carboxamide (**12e**). **12e** was synthesized from **11** (0.1 g, 0.286 mmol), K₂CO₃ (79 mg, 0.572 mmol), and 1-(bromomethyl)-3-fluorobenzene (42 µL, 0.344 mmol). Orange solid, 23% yield, carbonize at 210 °C. ¹H NMR (400 MHz, DMSO-*d*₆) δ 8.70 (s, 1H, CH), 8.41 (d, *J* = 7.5 Hz, 1H, NH), 8.36 (s, 1H, Ph-H), 7.39 (q, *J* = 7.5 Hz, 1H, Ph-H), 7.21–7.09 (m, 3H, Ph-H), 3.91–3.78 (m, 1H, CH), 3.71–3.53 (m, 2H, CH₂), 2.87–2.72 (m, 2H, CH₂), 2.43–2.14 (m, 2H, CH₂), 1.94–1.82 (m, 2H, CH₂), 1.61–1.46 (m, 2H, CH₂). HRMS *m/z* C₂₂H₂₀FN₃O₇: calcd 457.1285, found 456.1146 [M – H]⁺.

4.1.5.6. *N*-(1-(3-chlorobenzyl)piperidin-4-yl)-7,8-dihydroxy-6-nitro-2-oxo-2H-chromene-3-carboxamide (**12f**). **12f** was synthesized from **11** (0.1 g, 0.286 mmol), K₂CO₃ (79 mg, 0.572 mmol), and 1-(bromomethyl)-3-chlorobenzene (45 µL, 0.344 mmol). Orange solid, 21% yield, carbonize at 200 °C. ¹H NMR (400 MHz, DMSO-*d*₆) δ 8.70 (s, 1H, CH), 8.40 (d, *J* = 7.6 Hz, 1H, NH), 8.36 (s, 1H, Ph-H), 7.40–7.27 (m, 4H, Ph-H), 3.88–3.78 (m, 1H, CH), 3.63–3.48 (m, 2H, CH₂), 2.79–2.70 (m, 2H, CH₂), 2.32–2.12 (m, 2H, CH₂), 1.86 (d, *J* = 9.9 Hz, 2H, CH₂), 1.62–1.45 (m, 2H, CH₂). ¹³C NMR (100 MHz, DMSO-*d*₆) δ 162.8, 161.6, 161.2, 161.1, 151.3, 149.5, 146.7, 138.0, 135.4, 133.4, 132.4, 130.5, 127.6, 127.1, 115.3, 108.7, 101.9, 99.9, 51.8, 38.7, 31.6. HRMS *m/z* C₂₂H₂₀ClN₃O₇: calcd 473.0990, found 472.8017 [M – H]⁺.

4.1.5.7. *N*-(1-(3-bromobenzyl)piperidin-4-yl)-7,8-dihydroxy-6-nitro-2-oxo-2H-chromene-3-carboxamide (**12g**). **12g** was synthesized from **11** (0.1 g, 0.286 mmol), K₂CO₃ (79 mg, 0.572 mmol), and 1-bromo-3-(bromomethyl)benzene (55 µL, 0.344 mmol). Orange solid, 22% yield, carbonize at 180 °C. ¹H NMR (400 MHz, DMSO-*d*₆) δ 8.70 (s, 1H, CH), 8.40 (d, *J* = 7.5 Hz, 1H, NH), 8.36 (s, 1H, Ph-H), 7.54 (s, 1H, Ph-H), 7.47 (d, *J* = 7.1 Hz, 1H, Ph-H), 7.38–7.27 (m, 2H, Ph-H), 3.90–3.77 (m, 1H, CH), 3.68–3.49 (m, 2H, CH₂), 2.85–2.72 (m, 2H, CH₂), 2.39–2.13 (m, 2H, CH₂), 1.87 (d, *J* = 10.3 Hz, 2H, CH₂), 1.61–1.48 (m, 2H, CH₂). ¹³C NMR (100 MHz, DMSO-*d*₆) δ 162.8, 161.7, 161.2, 161.1, 149.5, 146.7, 138.0, 132.5, 130.9, 128.6, 127.1, 122.1, 120.9, 114.0, 108.7, 103.9, 101.9, 51.7, 38.7, 31.2. HRMS *m/z* C₂₂H₂₀BrN₃O₇: calcd 517.0485, found 516.0332 [M – H]⁺.

4.2. In vitro anti-HIV assay

The anti-HIV activity and cytotoxicity of synthesized derivatives were evaluated in MT-4 cell cultures using the MTT method, with wild-type HIV-1 strain IIIB, and mutant strains containing single amino acid substitutions in the viral RT (L100I, K103 N, E138K, Y181C and Y188L), or double-mutants (V106A/F227L and RES056), as well as the HIV-2 strain ROD [32]. Stock solutions (10 × final concentration) of test compounds were added in 25 µL volumes to two series of triplicate wells to allow simultaneous evaluation of the effects on mock- and HIV-infected cells. Using a Biomek 3000 robot (Beckman Instruments, Fullerton, CA), serial five-fold dilutions of the test compounds (final 200 µL volume per well) were made directly in flat-bottomed 96-well microtiter trays, including untreated control HIV-1 and mock-infected cell samples for each sample. HIV-1 strains stock (50 µL at 100–300 CCID₅₀) or culture medium was added to either the infected or mock-infected wells of the microtiter tray. Mock-infected cells were used to evaluate the effect of compounds on uninfected cells to assess cytotoxicity. Exponentially growing MT-4 cells were centrifuged for 5 min at 1000 rpm and the supernatant was discarded. The MT-4 cells were resuspended at 6 × 10⁵ cells/mL, and 50 µL aliquots were transferred to the microtiter tray wells. At five days after infection, the viability of mock- and HIV-infected cells was determined spectrophotometrically with the MTT assay.

This assay is based on the reduction of yellow-colored MTT (Acros Organics, Geel, Belgium) by mitochondrial dehydrogenase of

metabolically active cells to form a blue-purple formazan that can be measured spectrophotometrically. The absorbances were read in an eight-channel computer-controlled photometer at wavelengths of 540 and 690 nm. All data were calculated using the median optical density (OD) value of three wells. The EC₅₀ was defined as the concentration of the test compound allowing 50% protection from viral cytopathogenicity. The CC₅₀ was defined as the compound concentration that reduced the absorbance of mock-infected cells by 50%.

4.3. Cell permeability assays

The permeability of compounds **DW-4** and **8a** was determined with the human colon epithelial cancer cell line, Caco-2, as previously described [38]. The rate of membrane transport for both compounds was measured and expressed as apparent permeability (P_{app}). Nadolol and metoprolol were used as controls in the assays.

4.4. HIV-1 RNase H inhibition assay

Wild-type HIV-1 BH10 reverse transcriptase (RT) was expressed in *E. coli* and purified as previously described [39,40]. RNase H activity was determined with template-primer 31Trna/21P [35]. Briefly, the synthetic RNA oligonucleotide 31Trna (5'-UUUUUUUUUAGGAUACAUUGGUUAAAAGUAU-3') was labeled at its 5' end with [γ-³²P]ATP (PerkinElmer) and T4 polynucleotide kinase (New England Biolabs), and purified with a mini Quick SpinTM column (Roche) before annealing to the DNA primer 21P (5'-ATACTTTAACCATATGTATCC-3'). Candidate RNase H inhibitors were available in 50% DMSO, and reactions in the presence or absence of inhibitor were performed as previously described [38]. Assays were carried out for 15 s at 37 °C with 20–40 nM HIV-1 RT in 16 µL of 50 mM Tris-HCl (pH 8.0), 50 mM NaCl, 5 mM MgCl₂, 25 nM ³²P-labeled template-primer, and 5% DMSO. Products of the hydrolytic reaction were separated by denaturing polyacrylamide gel electrophoresis, and quantified by phosphorimaging as described [35,38]. IC₅₀ values (µM) were determined from dose-response curves after calculating the amount of cleaved substrate in the absence of inhibitor (5% DMSO) and in the presence of drug at concentrations in the range of 0.2–100 µM.

4.5. Molecular modeling

The molecular structure of compound **8a** was sketched using the Molecular Builder module implemented in Maestro (Maestro, Schrodinger, LLC, New York, NY, 2019) and then preprocessed with LigPrep (LigPrep, Schrodinger, LLC, New York, NY, 2019). Multiple protonation and tautomerization states at pH of 7.0 ± 2.0 were requested. Docking experiments were performed employing the crystal structure of a hydroxypyridone carboxylic acid active-site RNase H inhibitor in complex with HIV-1 RT (PDB ID: 5J1E). The protein setup was carried out using the Protein Preparation Wizard implemented in Maestro. Crystallographic water molecules were removed; hydrogen atoms were added to the protein consistent with the neutral physiologic pH and ensuring all other atoms positions remained fixed. The centroid of the x-ray ligand was defined as the grid box. van der Waals radius scaling factor 1.00, partial charge cutoff 0.25, and OPLS3e force field were used for receptor grid generation. Docking was carried out using the Ligand Docking module with extra precision. Each generated conformation of **8a** was subsequently docked and scored, and the conformation with the highest score was chosen as the final result. Docking was validated by measuring the RMSD between the predicted conformation of **8a** and that of the RNase H inhibitor found in the crystal structure 5J1E.

Declaration of competing interest

The authors declare that they have no known competing financial interests or personal relationships that could have appeared to influence the work reported in this paper.

Acknowledgments

We gratefully acknowledge financial support from the National Natural Science Foundation of China (NSFC Nos. 81973181, 81903453), Shandong Provincial Key research and development project (Nos. 2019JZZY021011), Shandong Provincial Natural Science Foundation (ZR2019BH011, ZR2020YQ61, ZR2020JQ31), Foreign cultural and educational experts Project (GXL20200015001), Qilu Young Scholars Program of Shandong University, the Taishan Scholar Program at Shandong Province, and KU Leuven (GOA 10/014). Work in Madrid was supported by the Spanish Ministry of Science and Innovation (grant PID2019-104176RB-I00/AEI/10.13039/501100011033), and an institutional grant of **Fundación Ramón Areces** (Madrid, Spain). The technical assistance of Mr. Kris Uyttersprot and Mrs. Kristien Erven, for the HIV experiments is gratefully acknowledged.

Appendix A. Supplementary data

Supplementary data to this article can be found online at <https://doi.org/10.1016/j.ejmech.2021.113769>.

References

- [1] UNAIDS, HIV Drug Resistance Report 2019, World Health Organization-UNAIDS, Geneva, 2019. <https://www.who.int/hiv/data/en>. (Accessed 26 June 2021).
- [2] D. Kang, F.X. Ruiz, Y. Sun, D. Feng, L. Jing, Z. Wang, T. Zhang, S. Gao, L. Sun, E. De Clercq, C. Pannecouque, E. Arnold, P. Zhan, X. Liu, 2,4,5-trisubstituted pyrimidines as potent HIV-1 NNRTIs: rational design, synthesis, activity evaluation, and crystallographic studies, *J. Med. Chem.* 64 (2021) 4239–4256.
- [3] M.E. Cilento, K.A. Kirby, S.G. Sarafianos, Avoiding drug resistance in HIV reverse transcriptase, *Chem. Rev.* 121 (2021) 3271–3296.
- [4] Y. Ma, E. Frutos-Beltrán, D. Kang, C. Pannecouque, E. De Clercq, L. Menéndez-Arias, X. Liu, P. Zhan, Medicinal chemistry strategies for discovering antivirals effective against drug-resistant viruses, *Chem. Soc. Rev.* 50 (2021) 4514–4540.
- [5] J.G. Moffat, J. Rudolph, D. Bailey, Phenotypic screening in cancer drug discovery – past, present and future, *Nat. Rev. Drug Discov.* 13 (2014) 588–602.
- [6] J.G. Moffat, F. Vincent, J.A. Lee, J. Eder, M. Prunotto, Opportunities and challenges in phenotypic drug discovery: an industry perspective, *Nat. Rev. Drug Discov.* 16 (2017) 531–543.
- [7] T.T. Ashburn, K.B. Thor, Drug repositioning: identifying and developing new uses for existing drugs, *Nat. Rev. Drug Discov.* 3 (2004) 673–683.
- [8] T.N. Jarada, J.G. Rokne, R. Alhaji, A review of computational drug repositioning: strategies, approaches, opportunities, challenges, and directions, *J. Cheminf.* 12 (2020) 46.
- [9] D. Kang, F.X. Ruiz, D. Feng, A. Pilch, T. Zhao, F. Wei, Z. Wang, Y. Sun, Z. Fang, E. De Clercq, C. Pannecouque, E. Arnold, X. Liu, P. Zhan, Discovery and characterization of fluorine-substituted dihydropyrimidine derivatives as novel HIV-1 NNRTIs with highly improved resistance profiles and low activity for the hERG ion channel, *J. Med. Chem.* 63 (2020) 1298–1312.
- [10] D. Kang, D. Feng, Y. Sun, Z. Fang, F. Wei, E. De Clercq, C. Pannecouque, X. Liu, P. Zhan, Structure-based bioisosterism yields HIV-1 NNRTIs with improved drug-resistance profiles and favorable pharmacokinetic properties, *J. Med. Chem.* 63 (2020) 4837–4848.
- [11] D. Kang, D. Feng, T. Ginex, J. Zou, F. Wei, T. Zhao, B. Huang, Y. Sun, S. Desta, E. De Clercq, C. Pannecouque, P. Zhan, X. Liu, Exploring the hydrophobic channel of NNIBP leads to the discovery of novel piperidine-substituted thiophene[3,2-d]pyrimidine derivatives as potent HIV-1 NNRTIs, *Acta Pharm. Sin. B* 10 (2020) 878–894.
- [12] D. Kang, T. Zhao, Z. Wang, D. Feng, H. Zhang, B. Huang, G. Wu, F. Wei, Z. Zhou, L. Jing, X. Zuo, Y. Tian, V. Poongavanam, J. Kongsted, E. De Clercq, C. Pannecouque, P. Zhan, X. Liu, Discovery of piperidine-substituted thiazolo 5,4-d pyrimidine derivatives as potent and orally bioavailable HIV-1 non-nucleoside reverse transcriptase inhibitors, *Commu. Chem.* 2 (2019) 74.
- [13] D. Kang, Z. Fang, B. Huang, X. Lu, H. Zhang, H. Xu, Z. Huo, Z. Zhou, Z. Yu, Q. Meng, G. Wu, X. Ding, Y. Tian, D. Daelemans, E. De Clercq, C. Pannecouque, P. Zhan, X. Liu, Structure-based optimization of thiophene[3,2-d]pyrimidine derivatives as potent HIV-1 non-nucleoside reverse transcriptase inhibitors with improved potency against resistance-associated variants, *J. Med. Chem.* 60 (2017) 4424–4443.
- [14] D. Kang, Z. Fang, Z. Li, B. Huang, H. Zhang, X. Lu, H. Xu, Z. Zhou, X. Ding, D. Daelemans, E. De Clercq, C. Pannecouque, P. Zhan, X. Liu, Design, synthesis, and evaluation of thiophene[3,2-d]pyrimidine derivatives as HIV-1 non-nucleoside reverse transcriptase inhibitors with significantly improved drug resistance profiles, *J. Med. Chem.* 59 (2016) 7991–8007.
- [15] D. Feng, A. Zhang, Y. Yang, P. Yang, Coumarin-containing hybrids and their antibacterial activities, *Arch. Pharm.* 353 (2020), e1900380.
- [16] S. Mishra, A. Pandey, S. Manvati, Coumarin: an emerging antiviral agent, *Heliyon* 6 (2020), e03217.
- [17] D. Pinto, A.M.S. Silva, Anticancer natural coumarins as lead compounds for the discovery of new drugs, *Curr. Top. Med. Chem.* 17 (2017) 3190–3198.
- [18] N. Bhattarai, A.A. Kumbhar, Y.R. Pokharel, P.N. Yadav, Anticancer potential of coumarin and its derivatives, *Mini Rev. Med. Chem.* (2021), <https://doi.org/10.2174/1389557521666210405160323>.
- [19] K.N. Venugopala, V. Rashmi, B. Odhav, Review on natural coumarin lead compounds for their pharmacological activity, *BioMed Res. Int.* 2013 (2013) 963248.
- [20] World Health Organization, World Health Organization Model List of Essential Medicines: 21st List 2019, World Health Organization, Geneva, 2019.
- [21] Y. Kashman, K.R. Gustafson, R.W. Fuller, J.H. Cardellina 2nd, J.B. McMahon, M.J. Currens, R.W. Buckheit Jr., S.H. Hughes, G.M. Cragg, M.R. Boyd, The calanolides, a novel HIV-inhibitory class of coumarin derivatives from the tropical rainforest tree, *Calophyllum lanigerum*, *J. Med. Chem.* 35 (1992) 2735–2743.
- [22] D. Du, X. Liu, Z. Zheng, P. Zhan, F. Zhang, Coumarin Amid Derivative and Application Thereof, Patent Application CN 107935976B, 2018.
- [23] L. Yang, Q. Yang, K. Zhang, Y.J. Li, Y.M. Wu, S.B. Liu, L.H. Zheng, M.G. Zhao, Neuroprotective effects of daphnetin against NMDA receptor-mediated excitotoxicity, *Molecules* 19 (2014) 14542–14555.
- [24] B. Zhou, J. Wang, G. Zheng, Z. Qiu, Methylated urolithin A, the modified ellagitannin-derived metabolite, suppresses cell viability of DU145 human prostate cancer cells via targeting miR-21, *Food Chem. Toxicol.* 97 (2016) 375–384.
- [25] F. Esposito, F.A. Ambrosio, R. Maleddu, G. Costa, R. Rocca, E. Maccioni, R. Catalano, I. Romeo, P. Eleftheriou, D.C. Karia, P. Tsiroides, N. Godvani, H. Pandya, A. Corona, S. Alcaro, A. Artese, A. Geronikaki, E. Tramontano, Chromenone derivatives as a versatile scaffold with dual mode of inhibition of HIV-1 reverse transcriptase-associated ribonuclease H function and integrase activity, *Eur. J. Med. Chem.* 182 (2019) 111617.
- [26] M. Zhu, L. Ma, J. Wen, B. Dong, Y. Wang, Z. Wang, J. Zhou, G. Zhang, J. Wang, Y. Guo, C. Liang, S. Cen, Y. Wang, Rational design and structure-activity relationship of coumarin derivatives effective on HIV-1 protease and partially on HIV-1 reverse transcriptase, *Eur. J. Med. Chem.* 186 (2020) 111900.
- [27] P. Wadhwa, P. Jain, S. Rudrawar, H.R.A. Jadhav, Quinoline, coumarin and other heterocyclic analogs based HIV-1 integrase inhibitors, *Curr. Drug Discov. Technol.* 15 (2018) 2–19.
- [28] Z. Xu, Q. Chen, Y. Zhang, C. Liang, Coumarin-based derivatives with potential anti-HIV activity, *Fitoterapia* 150 (2021) 104863.
- [29] H. Zhai, N. Neamati, H. Hong, A. Mazumder, S. Wang, S. Sunder, G.W. Milne, Y. Pommier, T.R. Burke Jr., Coumarin-based inhibitors of HIV integrase, *J. Med. Chem.* 40 (1997) 242–249.
- [30] L. Tao, Y.T. Zhuo, Z.H. Qiao, J. Li, H.X. Tang, Q.M. Yu, Y.Y. Liu, Y.P. Liu, Prenylated coumarins from the fruits of *Artocarpus heterophyllus* with their potential anti-inflammatory and anti-HIV activities, *Nat. Prod. Res.* (2021), <https://doi.org/10.1080/14786419.2021.1913590>.
- [31] Y.P. Liu, G. Yan, Y.T. Xie, T.C. Lin, W. Zhang, J. Li, Y.J. Wu, J.Y. Zhou, Y.H. Fu, Bioactive prenylated coumarins as potential anti-inflammatory and anti-HIV agents from *Clausena lenis*, *Bioorg. Chem.* 97 (2020) 103699.
- [32] C. Pannecouque, D. Daelemans, E. De Clercq, Tetrazolium-based colorimetric assay for the detection of HIV replication inhibitors: revisited 20 years later, *Nat. Protoc.* 3 (2008) 427–434.
- [33] X. Wang, P. Gao, L. Menéndez-Arias, X. Liu, P. Zhan, Update on recent developments in small molecular HIV-1 RNase H inhibitors (2013–2016): opportunities and challenges, *Curr. Med. Chem.* 25 (2018) 1682–1702.
- [34] E. Tramontano, A. Corona, L. Menéndez-Arias, Ribonuclease H, an unexploited target for antiviral intervention against HIV and hepatitis B virus, *Antivir. Res.* 171 (2019) 104613.
- [35] M. Alvarez, T. Matamoros, L. Menéndez-Arias, Increased thermostability and fidelity of DNA synthesis of wild-type and mutant HIV-1 group O reverse transcriptases, *J. Mol. Biol.* 392 (2009) 872–884.
- [36] D. Kang, H. Zhang, Z. Wang, T. Zhao, T. Ginex, F.J. Luque, Y. Yang, G. Wu, D. Feng, F. Wei, J. Zhang, E. De Clercq, C. Pannecouque, C.H. Chen, K.-H. Lee, N.A. Murugan, T.A. Steitz, P. Zhan, X. Liu, Identification of dihydrofuro[3,4-d]pyrimidine derivatives as novel HIV-1 non-nucleoside reverse transcriptase inhibitors with promising antiviral activities and desirable physicochemical Properties, *J. Med. Chem.* 62 (2019) 1484–1501.
- [37] J. Kankanala, K.A. Kirby, F. Liu, L. Miller, E. Nagy, D.J. Wilson, M.A. Parniak, S.G. Sarafianos, Z. Wang, Design, synthesis, and biological evaluations of hydroxypyridonecarboxylic acids as inhibitors of HIV reverse transcriptase associated RNase H, *J. Med. Chem.* 59 (2016) 5051–5062.
- [38] P. Gao, X. Cheng, L. Sun, S. Song, M. Álvarez, J. Luczkowiak, C. Pannecouque, E. De Clercq, L. Menéndez-Arias, P. Zhan, X. Liu, Design, synthesis and biological evaluation of 3-hydroxyquinazoline-2,4-(1H,3H)-diones as dual inhibitors of HIV-1 reverse transcriptase-associated RNase H and integrase,

- Bioorg. Med. Chem. 27 (2019) 3836–3845.
- [39] J. Boretto, S. Longhi, J.M. Navarro, B. Selmi, J. Sire, B. Canard, An integrated system to study multiply substituted human immunodeficiency virus type 1 reverse transcriptase, *Anal. Biochem.* 292 (2001) 139–147.
- [40] T. Matamoros, J. Deval, C. Guerreiro, L. Mulard, B. Canard, L. Menéndez-Arias, Suppression of multidrug-resistant HIV-1 reverse transcriptase primer unblocking activity by alpha-phosphate-modified thymidine analogues, *J. Mol. Biol.* 349 (2005) 451–463.